Chemical and Biological Technologies in Agriculture

RESEARCH

Open Access

Elimination of *Curtobacterium* sp. strain A7_M15, a contaminant in *Prunus* rootstock tissue culture production, using reduced graphene oxide–silver–copper and silver–selenium nanocomposites

Dorota Tekielska[1*], Jakub Pečenka[1], Eliška Hakalová[1], Jana Čechová[1], Zuzana Bytešníková[2], Lukáš Richtera[2], Tomáš Kiss[3], Aleš Eichmeier[1] and Miroslav Baránek[1]

Abstract

Background Bacterial contamination poses a high risk to the successful establishment and maintenance of plant tissue cultures. The aim of this study was to identify the isolates representing the frequent bacterial contaminants of *Prunus* rootstock tissue cultures and to determine the most effective concentration of nanomaterials for *Curtobacterium* sp. strain A7_M15 elimination without a negative impact on explants.

Results Six *Curtobacterium* sp. strains were isolated and identified, and the whole-genome sequence was obtained for strain A7_M15. Two nanocomposites, reduced graphene oxide–copper–silver and silver–selenium, with the highest bactericidal activity were selected for elimination of *Curtobacterium* sp. contamination in Gisela 5 rootstock tissue cultures. Both nanocomposites showed 100% inhibition of bacterial plaque formation on culture medium at concentrations of 100, 200 and 400 mg L^{-1} Ag (2 ×–8 × MBC). The quantity of *Curtobacterium* sp. on culture medium assessed using cfu enumeration was reduced by 92% and 74% in comparison to the positive control after treatment with reduced graphene oxide–silver–copper and silver–selenium at a concentration of 200 mg L^{-1} Ag, respectively. None of the tested concentrations resulted in a decrease in *Curtobacterium* sp. quantity in explants. *Curtobacterium* sp. was detected in donor Gisela 5 plants, indicating an endophytic character of this bacterium. The dry weight of explants was not negatively affected by the application of nanocomposites regardless of concentration, and no detrimental effect of either nanocomposite at 100 or 200 mg L^{-1} Ag on the surface covered by plants was observed.

Conclusions Reduced graphene oxide–silver–copper and silver–selenium nanocomposites at 200 mg L^{-1} Ag effectively limited the *Curtobacterium* sp. presence in micropropagated *Prunus* rootstock without causing phytotoxicity; therefore, those treatments could be offered as prevention with a high activity against bacterial contamination in plant tissue cultures.

Keywords Nanomaterial, Nanocomposite, Reduced graphene oxide, Silver, *Curtobacterium*, *Prunus*, Contamination, Tissue culture, Micropropagation

*Correspondence:
Dorota Tekielska
dorota.tekielska@mendelu.cz
Full list of author information is available at the end of the article

Graphical Abstract

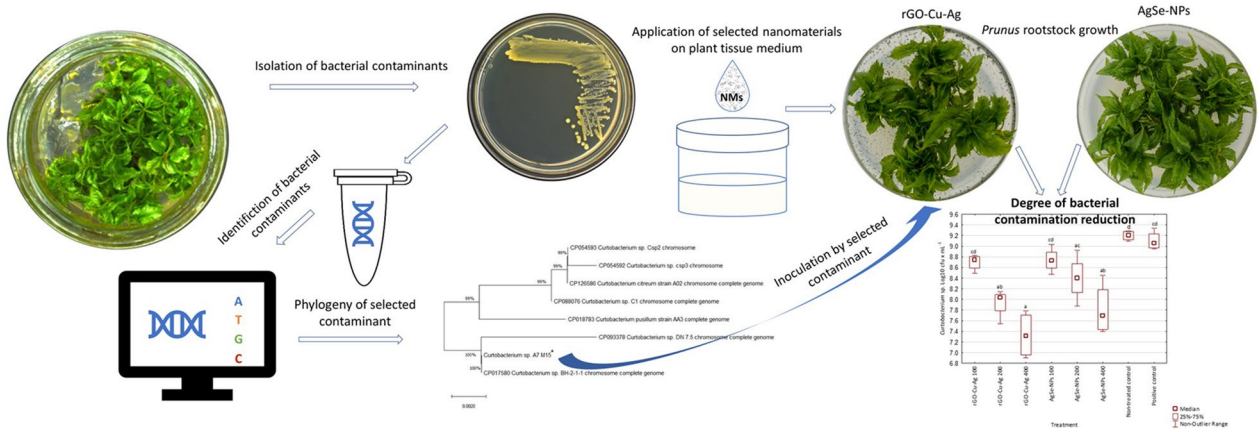

Background

The establishment of plant tissue cultures requires aseptic conditions; however, microbial contamination often occurs during the manipulation of explants. Among various microorganisms, bacteria are described as a serious risk in every application of plant in vitro culture techniques [1, 2]. The problem of undesired microorganisms contaminating tissue cultures is present both in commercial and scientific laboratories. Efficient production can be achieved when losses due to microbiological contamination do not exceed 2% per subculture [1, 2]. Except for introducing safety practices during all steps of in vitro plant production, there is a need to use antimicrobial substances. Establishment of tissue culture requires disinfection of initial plant material, and for this purpose, mercuric chloride, sodium and calcium hypochlorite, ethanol or antibiotics are routinely used [3–5]. Despite the effective elimination of microorganisms during this process, some contamination may occur during further manipulation with cultures from external sources or internal latent bacteria [6, 7].

Treatments of tissue cultures in which a problem with bacterial contamination has been recorded are mainly limited to antibiotics, which may show a phytotoxic effect [5, 8] or adaptive resistance may begin to appear [9]. As an alternative to antibiotics, the use of the generally recorded antimicrobial effect of nanoparticles is theoretically offered [10]. Regarding plant tissue cultures, nanomaterials have already been used, applied both for disinfection during in vitro culture establishment and for maintaining a contamination-free culture [3, 11]. Compounds or elements with already confirmed antimicrobial effects may exhibit effectiveness at lower concentrations if applied in the form of nanomaterials [12]. The most widely used nanomaterials with antimicrobial activity are silver nanoparticles [13–15], but zinc and copper at the nanoscale can also show high efficiency against microorganisms [16, 17]. Silver nanoparticles decreased microbial contamination when used as a soaking treatment and additive to medium in micropropagated *Pennisetum alopecuroides* Spreng. [3]. Bacterial contaminants were removed from *Valeriana officinalis* L. nodal explants [18] and tissue culture of *Aldrovanda vesiculosa* L. [19] using silver nanomaterials. To a lesser extent, copper nanomaterials have also been successfully used in plant in vitro cultures, as in the case of different explants of *Begonia*×*tuberhybrida* Voss, where the treatment stimulated maturation of somatic embryos [20, 21].

Graphene materials, such as reduced graphene oxide (rGO), are also used for studying antibacterial effects, but the results are not unequivocal [22–25]. Reinforcement of the antimicrobial activity of rGO can be achieved by its rearrangement, which includes metal and metal oxide structures [23]. The reduced graphene oxide nanocomposite with copper and silver nanoparticles was effective against *Xanthomonas euvesicatoria* in an in vitro assay, as well as a protective agent on tomato plants [26]. Silver nanoparticles were deposited on rGO to increase the effect against *Staphylococcus aureus* and *S. epidermidis* [21]. The activity of rGO loaded with sulfur and selenium nanoparticles was tested against *S. aureus* and *Enterococcus faecalis,* and rGO-S/Se nanoparticles showed the strongest effectivity against both Gram-positive pathogens [27].

The effective elimination of bacterial contaminants in in vitro cultures needs to be, in some cases, preceded by the identification of present isolates, which can help to adjust proper measures to avoid their occurrence [4, 28, 29]. Bacteria contaminating different types of tissue cultures often originate from insufficient precautions during initiation and maintenance of explants or are present in the plant parts as endophytes and persist even after applied sterilization [28, 30, 31]. In a previous study, we identified various bacterial genera contaminating *Prunus* rootstock cultures in commercial production [32]. High-throughput sequencing allowed us to identify 11 species: *Acinetobacter, Lactobacillus, Methylobacterium, Roseomonas, Microbacterium, Mycobacterium, Curtobacterium, Acidovorax, Magnetospirillum, Chryseobacterium* and *Ralstonia*. In another study analyzing contaminants of micropropagated *Prunus yedoensis,* two genera were identified and described as endophytes: *Pantoea* spp. and *Curtobacterium* spp. [5]. Romadanova et al. [28] detected endophytic *Bacillus megaterium* in apple shoot in vitro cultures.

Species belonging to the *Curtobacterium* genus are Gram-positive, obligately aerobic chemoorganotrophs in the family *Microbacteriaceae*, phylum *Actinobacteria* [33]. For example, in this genus, the quarantine *Curtobacterium flaccumfaciens* pv. *flaccumfaciens* can be found, which is an important emerging disease threatening the edible legume industry around the globe [34]. Members of the genus *Curtobacterium* were also determined to be the most abundant bacteria participating in the degradation of organic matter within leaf litter communities. Their very well-established genomic background customized for the degradation of plant polysaccharides such as cellulose was emphasized [35], which may evoke the assumption that their presence in in vitro cultures might therefore be undesirable.

In the present study, we isolated and identified bacterial contaminants present within *Prunus* rootstock tissue cultures collected from two different laboratories. Moreover, we tested the antibacterial activity of various types of nanomaterials based on reduced graphene oxide, silver, copper, zinc and selenium against the most abundant *Curtobacterium* sp. represented by the newly sequenced strain A7_M15. The most effective nanomaterials were applied in the tissue cultures during the multiplication procedure to eliminate the contamination.

Methods

Plant in vitro cultures with bacterial contamination

Plant in vitro cultures with visible bacterial contamination were obtained from two laboratories in the Czech Republic: Mendeleum-Department of Genetics, Faculty of Horticulture in Lednice, Mendel University in Brno and Vitrotree by Battistini in Šakvice. Samples from six prunus rootstock genotypes were collected: GF-677 (*Prunus persica* × *Prunus dulcis*), Gisela 5 (*Prunus cerasus* × *Prunus canescens*), Adesoto (*Prunus insititia*), Ishtara ((*Prunus cerasifera*×*P. persica*)×*Prunus salicina*), Myrobalan 29C (*P. cerasifera*), and Torinel (*Prunus domestica*). All tissue cultures were grown on DKW/Juglans medium (Duchefa Biochemie, Haarlem, Netherlands).

Isolation of bacterial contaminants

To obtain single colonies, bacteria present on culture media were sampled using a sterile 10 µL inoculation loop. Samples were transferred to 2 mL sterile tubes containing Luria broth (LB, HiMedia, Mumbai, India) and incubated for 2 h at 28 ℃ with agitation (90 rpm) on an orbital shaker (Biosan, Riga, Latvia). Subsequently, samples were tenfold serially diluted in sterile phosphate buffered saline (PBS) from 10^{-1} to 10^{-4}, and 100 µL of each sample was spread on Petri dishes containing Luria agar (LA, HiMedia, Mumbai, India). Petri dishes were incubated at 28 ℃ for 24–72 h until bacterial colonies were visible. Single-colony isolates were prepared from morphologically distinct colonies by the streak plate method on LA medium. The obtained isolates were stored in 25%

Table 1 Concentrations of nanomaterials used for minimum bactericidal concentration determination

Nanomaterial concentration (mg L^{-1})							
rGO-Cu	rGO-Zn	rGO-Cu-Ag		AgSe-NPs		AgNPs_1	AgNPs_2
Cu	Zn	Ag	Cu	Ag	Se	Ag	Ag
50	50	25	16.25	25	15.42	25	25
100	100	50	32.50	50	30.83	50	50
500	500	100	65.00	100	61.67		
600	600						
700	700						
800	800						
900	900						
1000	1000						

glycerol at -80 ℃ in the collection of the Mendeleum Department of Genetics.

Identification of bacterial isolates

Bacterial suspensions were prepared from the obtained isolates in sterile PBS at a concentration of 1×10^8 cfu mL^{-1}. From each suspension, 500 µL was centrifuged at 11 000 × *g* for 5 min (Andreas Hettich GmbH & Co. KG, Tuttlingen, Germany), the supernatant was removed, and the pellet was used for DNA extraction using a NucleoSpin Tissue kit (Macherey–Nagel, Dueren, Germany) according to the manufacturer's protocol for bacteria. The concentration and purity of extracted DNA samples were measured using a Spectrostar Nano spectrophotometer (BMG Labtech, Ortenberg, Germany). For identification of the obtained bacterial isolates, PCR was performed using the universal 16S rRNA primer pair: S-D-Bact-0341-b-S-17 (5′-CCTACG GGNGGCWGCAG-3′) and S-D-Bact-0785-a-A-21 (5′-GACTACHVGGGTATCTAATCC-3') [36]. Reactions of a 20 µL volume consisted of 1 U GoTaq® G2 polymerase (Promega, Madison, WI, USA), 1 × Colorless flexi buffer (Promega, Madison, WI, USA), 1.5 mM $MgCl_2$ (Promega, Madison, WI, USA), 0.1 mM dNTPs, 0.5 µM of each primer, 50 ng of DNA per sample and PCR grade water. PCR conditions consisted of 95 ℃ for 3 min of initial denaturation and 30 cycles of 95 ℃ for 2 min, 50 ℃ for 25 s, and 72 ℃ for 2 min followed by 72 ℃ for 5 min as a final extension step. PCR products were separated in a 1.2% agarose gel by electrophoresis, visualized with Midori Green (Nippon Genetics, Dueren, Germany) in an Azure 600 imaging system (Azure Biosystems, Dublin, CA, USA) and purified using a NucleoSpin Gel and PCR Clean-up kit (Macherey–Nagel, Dueren, Germany) according to the manufacturer's protocol. Amplicons were sequenced using the Mix2Seq service (Eurofins Genomics, Ebersberg, Germany), and sequences were compared with the BLASTn NCBI database.

Identification of the *Curtobacterium* sp. A7_M15 isolate using a metabolic phenotyping assay

For the analysis of the *Curtobacterium* sp. A7_M15 isolate phenotypic fingerprint, the Biolog Microstation System and the GEN III MicroPlate test panel (Biolog Inc., Hayward, CA, USA) were used according to the manufacturer's protocol. The microplate was incubated for 48 h and read on the Biolog automated microbial analysis system software (MicroLog Secure 6.2).

Whole genome sequencing of *Curtobacterium* sp. A7_M15 isolate and data processing

For the genomic sequencing, the same DNA as for 16S-based identification was used, i.e., extracted using NucleoSpin Tissue kit (Macherey–Nagel, Dueren, Germany) according to the manufacturer's protocol for bacteria. The genomic DNA was randomly sheared into short fragments. The obtained fragments were end repaired, A-tailed and further ligated with an Illumina adapter. The fragments with adapters were PCR amplified, size selected, and purified. The library was checked with Qubit and real-time PCR for quantification and a bioanalyzer for size distribution detection. The quantified library was sequenced on an Illumina platform according to the effective library concentration and data amount needed. The reads containing low-quality bases (mass value ≤ 20) over a certain percentage (the default was 40%) were removed. The number of N in reads beyond a certain proportion (the default was 10%) was removed. Some reads, the overlap between them and the adapter, which exceeded a certain threshold (the default was 15 bp) and had less than 3 mismatches between them, were removed. After Clean Data were obtained, the assembly was first performed using SOAPdenovo (version 2.04) [37–41] assembly software and finally using CISA software [42] for integration. All the protein sequences were aligned to the genome sequences using BLAST, and then GeneWise was used to predict gene structure-based reliable alignments (evalue < 1×10^{-5}). Then, the coding genes were predicted by Augustus [38] with homologous evidence.

Nanomaterials used against *Curtobacterium* sp. A7_M15 in in vitro assays

Six nanoparticles and nanocomposites selected for the experiment were provided by the Department of Chemistry and Biochemistry, Mendel University in Brno, Czech Republic. Three nanocomposites were based on reduced graphene oxide combined with zinc (rGO-Zn) [43], copper and copper with silver (rGO-Cu and rGO-Cu-Ag) [26], one nanocomposite was based on silver and selenium (AgSe-NPs) [44] and two nanoparticles were based on silver (AgNPs_1, AgNPs_2) [45]. All used nanomaterials have been characterized using standard procedures, and their properties can be verified in the corresponding references. Stock solutions of nanomaterials were stored at 4 ℃ in the dark (Additional file 1: Fig. S1 and Fig. S2). Solutions of nanomaterials for all assays were prepared with distilled deionized water.

Minimum bactericidal concentrations of nanomaterials

The effectiveness of nanomaterials was tested using the bacterial suspension of the isolate of *Curtobacterium* sp. A7_M15, which was retrieved from cryo-preservation and grown on LA medium at 28 ℃ for 24 h. Subsequently, a liquid culture was prepared by inoculating LB medium with a single colony and cultivating for 24 h at 28 ℃

on an orbital shaker (150 rpm, Biosan, Riga, Latvia). For the minimum bactericidal concentration (MBC) determination, a suspension of *Curtobacterium* sp. A7_M15 was treated with the tested nanomaterials at the scale of concentrations presented in Table 1. Stock solutions of AgNPs_1 and AgNPs_2 contained 100 mg L^{-1} of silver; therefore, the maximal concentration used was 50 mg L^{-1}. The bacterial suspension in LB was adjusted to a final concentration of approximately 1×10^6 cfu mL^{-1} based on optical density (OD_{600}) using a Spectrostar Nano spectrophotometer (BMG Labtech, Ortenberg, Germany). Subsequently, 500 µL of nanomaterial solution was mixed with 500 µL of bacterial suspension in a 2 mL microcentrifuge tube and incubated on an orbital shaker (Biosan, Riga, Latvia) (24 h, 28 ℃, 150 rpm). A positive control was prepared by replacing the nanomaterial solution with the same volume of sterile deionized water. After incubation, 5 µL of bacterial suspension treated with the tested nanomaterials and positive control were pipetted in triplicate on LA plates and incubated at 28 ℃ for 24 h. The concentration that prevented bacterial growth was considered the MBC.

Elimination of bacterial contamination in plant tissue cultures

Based on a bactericidal assay, two of the most effective nanomaterials, rGO-Cu-Ag and AgSe-NPs, were selected for the treatment of plant tissue cultures against the *Curtobacterium* sp. A7_M15 isolate. First, both nanomaterials at the minimum bactericidal concentration (1×MBC) determined using bacterial suspension were tested on plant in vitro cultures, and subsequently, concentrations of 2×MBC, 4×MBC and 8×MBC were used to increase effectivity. The effectiveness of nanomaterials in eliminating bacterial contamination was tested on Gisela 5 rootstock in vitro cultures.

Nanomaterial application, bacterial inoculation and establishment of plant tissue cultures

DKW/Juglans medium was prepared in a 50 mL volume per glass container. Nanomaterials at selected concentrations were applied on the surface of solid medium at a volume of 2 mL, spread thoroughly by rotating the glass container and incubated in sterile conditions until the surface was dry. Subsequently, the medium was inoculated with bacterial suspension at a concentration of 1×10^6 cfu mL^{-1} in sterile PBS by pipetting 5 µL of suspension on 5 points and left to dry. Five single node shoot explants of Gisela 5 per glass container were transferred on treated culture medium and placed just at points of inoculation with bacterial suspension. The remaining tissues of donor plant material were stored at -40 ℃. To compare with the standard antibacterial agent used for the control of microbial contamination in tissue cultures, ProClin™ 200 (Sigma–Aldrich, St. Louis, MO, USA) was applied to the media before sterilization at a concentration of 0.05% (v/v), as recommended by the manufacturer. For the positive control, the nanomaterial treatment was replaced with sterile deionized water, while non-treated control was established by replacing nanomaterials with sterile deionized water and bacterial inoculum with sterile PBS buffer. The possible phytotoxic effect of nanomaterials on explants was evaluated by applying nanomaterials at the tested concentrations and replacing the bacterial inoculum with sterile PBS. For each treatment, three replicates were established. In vitro cultures were grown at 22 ℃ with a 16 h light/8 h dark photoperiod for 3 weeks.

Evaluation of bacterial contamination and quantification of *Curtobacterium* sp. on tissue culture medium

Before bacterial growth evaluation, each container with explants was recorded by a Nikon D3200 camera (Nikon, Minato, Japan), and the area covered by plants was

Fig. 1 Bacterial contamination present on Gisela 5 rootstock culture medium (the *Curtobacterium* sp. A7_M15 isolate source sample) (**a**, **b)** and isolated *Curtobacterium* sp. A7_M15 on Luria agar (**c)**

measured using FIJI software (LOCI, Wisconsin, USA). Subsequently, explants were removed from the tissue culture medium at the end of the 3-week growth period, and the presence or absence of bacterial plaque was determined at each inoculation point. The percentage of bacterial growth inhibition was calculated based on the number of plaques per container. Five explants from each glass container were pooled, weighed for plant mass evaluation and stored for DNA extraction. The surface of the medium was washed with 5 mL of sterile PBS buffer, and the whole volume was collected in sterile 5 mL tubes. One hundred microliters of collected sample were serially diluted tenfold up to 10^{-5} and spread on LA medium. Petri dishes were incubated at 28 ℃ for 24 h, and bacterial colonies were enumerated. Five hundred microliters of each sample were used for DNA extraction with a NucleoSpin Tissue kit (Macherey–Nagel, Dueren, Germany) according to the manufacturer's protocol.

Absolute quantification was carried out using a qTOWER real-time PCR cycler (Analytik Jena, Jena, Germany) using a specific primer pair for the genus *Curtobacterium*: curto-F2 (5′-GAAATGGTGTTATGG CCGGAT-3′) and curto D-R (5′-ACGGGTTAACCT CGCCACA-3′) [46]. One reaction consisted of 1 × Luna Universal qPCR Master Mix (New England Biolabs, Ipswich, MA, USA), 0.4 µM of each primer, 2 µL of DNA and PCR grade water added to a 20 µL volume. Each sample was tested in duplicate. PCR conditions consisted of 95 ℃ for 1 min for initial denaturation and 40 cycles of 95 ℃ for 30 s, 65 ℃ for 10 s, and 72 ℃ for 20 s and read on the FAM channel. The specificity of PCR products was verified by melting analysis after cycling. qPCRsoft 3.4 software (Analytik Jena, Jena, Germany) was used for fluorescence acquisition and melt analysis.

Prior to calculation of absolute quantities, the standard curve was prepared. First, *Curtobacterium sp.* A7_M15 cultured in LB medium (24 h, 28 ℃) was collected by centrifugation (4500 × *g*, 10 min). The pellet was resuspended in PBS and adjusted to approximately 3.0 OD_{600} using a Spectrostar Nano spectrophotometer (BMG Labtech, Ortenberg, Germany). The exact number of cfu mL^{-1} was obtained after enumeration of colonies formed from tenfold serial dilutions of 3.0 OD_{600} suspension after culturing on LA medium at 28 ℃ for 24 h. In parallel, bacterial cells were collected from 1 mL of 3.0 OD_{600} suspension by centrifugation (8000 × *g*, 5 min), and the pellet was subjected to DNA extraction using a NucleoSpin Tissue kit (Macherey–Nagel, Dueren, Germany) according to the manufacturer's instructions. The DNA was diluted in a solution of DNA extracted using NucleoSpin Tissue kit (Macherey–Nagel, Dueren, Germany from *Curtobacterium spp.*-negative plants to create a 6-point tenfold serial dilution, which was used to create a standard curve. The standard curve was established in qPCRsoft 3.4 software (Analytik Jena, Jena, Germany), where the slope (k) of the linear regression line between the Ct values and a log value of bacterial concentration was used to calculate the amplification

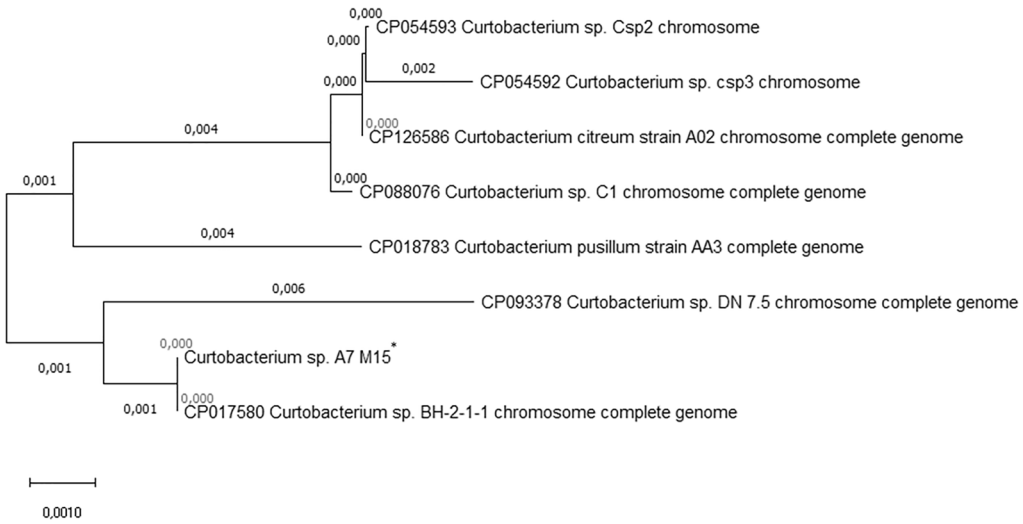

Fig. 2 The evolutionary history was inferred by using the maximum likelihood method and Tamura–Nei model [47]. The tree with the highest log likelihood (– 1832.07) is shown. Initial tree(s) for the heuristic search were obtained automatically by applying neighbor-join and BioNJ algorithms to a matrix of pairwise distances estimated using the Tamura–Nei model and then selecting the topology with superior log likelihood value. The tree is drawn to scale, with branch lengths measured in the number of substitutions per site. This analysis involved 8 nucleotide sequences. There were a total of 1196 positions in the final dataset. Evolutionary analyses were conducted in MEGA X [48]. The tree is based on a 1190-bp-long 16S rDNA sequence. *Curtobacterium* sp. A7_M15 is highlighted by an asterisk

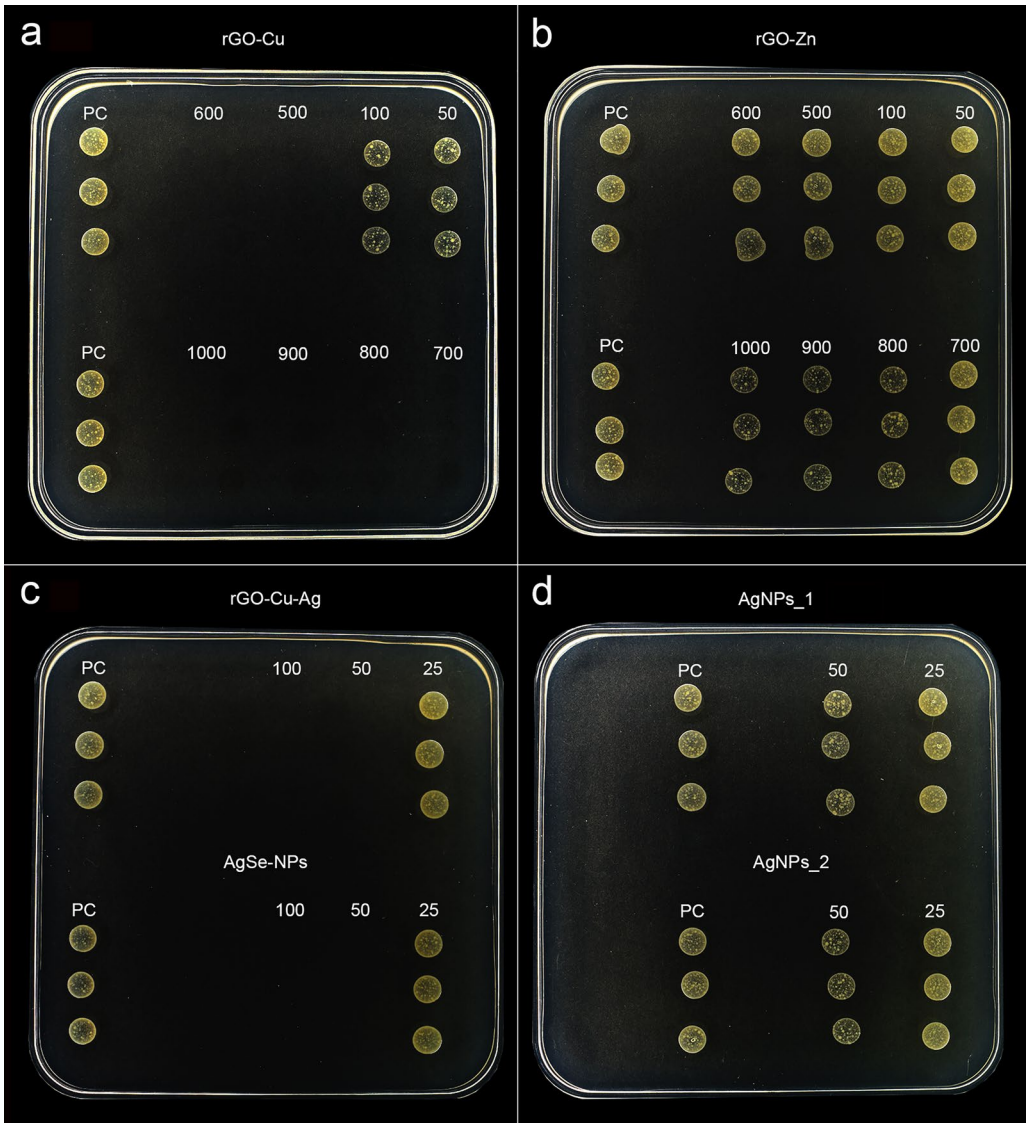

Fig. 3 Minimum bactericidal concentrations of tested nanomaterials against *Curtobacterium* A7_M15. Bacterial growth after treatment with rGO-Cu (**a**) and rGO-Zn (**b**) at 50–1000 mg L^{-1} Cu/Zn, rGO-Cu-Ag and AgSe-NPs at 25–100 mg L^{-1} Ag (**c**), and AgNPs_1 and AgNPs_2 at 25–50 mg L^{-1} Ag (**d**) compared with the positive control (PC)

efficiency (E). The squared regression coefficient (R^2) was determined after linear regression. Absolute quantities were expressed as *Curtobacterium sp.* A7_M15 cfu per whole DNA sample (referred as sample).

DNA extraction and quantification of *Curtobacterium* sp. in donor plant material and explants

During multiplication, each explant was assigned to donor plants, which allowed us to determine whether *Curtobacterium* sp. was already present during culture establishment. Donor plants, as well as five pooled samples from each replicate, were homogenized with 5 mL of PBS in extraction bags (Bioreba, Reinach, Switzerland), and 500 µL of homogenate was used for DNA extraction with a NucleoSpin Tissue kit (Macherey–Nagel, Dueren, Germany) according to the manufacturer's protocol. Detection (donor plants) and absolute quantification (explants after treatment) of *Curtobacterium* sp. were conducted using the same qPCR protocol as employed for quantification on the culture medium and the absolute quantities were expressed as *Curtobacterium* sp. A7_M15 cfu per gram of plant tissue.

Table 2 Effect of tested nanomaterials on inhibition (%) of bacterial plaque formation on inoculated plant tissue media

Treatment	Concentration (mg L^{-1} of Ag)	Inhibition (%)
rGO-Cu-Ag	50	45
	100	100
	200	100
	400	100
AgSe-NPs	50	30
	100	100
	200	100
	400	100
ProClin 200™	0.5%	10
Non-treated control	–	0
Positive control	–	0

Statistical analysis

Variant analysis and Tukey's test were carried out to analyze the obtained data and to determine the significant differences in the parameters of plants and *Curtobacterium* sp. quantity after the treatments at $p < 0.05$. The statistical software package STATISTICA (version 14.0.0.15, TIBCO Software Inc., Palo Alto, CA, USA) was used for all statistical analyses.

Results

Identification of bacteria isolated from contaminated tissue cultures

Bacterial contaminants present in in vitro cultures of 6 *Prunus* rootstock genotypes (GF 677, Gisela 5, Adesoto, Ishtara, Myrobalan 29C, Torinel) were isolated and identified based on 16S rRNA sequencing. In this way, 11 different bacterial isolates were obtained and identified, and *Curtobacterium* sp. with a total of six isolates was the most numerous. In all six isolates, the sequenced DNA fragments of 16S rRNA were identical. The 16S rRNA sequences of six *Curtobacterium* sp. isolates were deposited in the NCBI database and are available through accession numbers OR474083 (M7), OR474084 (M9), OR474085 (M14), OR474086 (A7_M15), OR474087 (M25), OR474088 (M27). NCBI BLASTn analysis of these sequences showed their identity with *Curtobacterium flaccumfaciens*, *C. luteum*, *C. oceanosedimentum* or *C. albidum*. As a representative of this group, the *Curtobacterium sp.* A7_M15 isolate was selected for further work. The *Prunus* rootstock Gisela 5 culture with visible contamination by *Curtobacterium* sp. A7_M15 and the isolated strain on Luria agar are presented in Fig. 1a–c. The metabolic phenotype profile of the *Curtobacterium* sp. A7_M15 isolate showed the highest similarity to

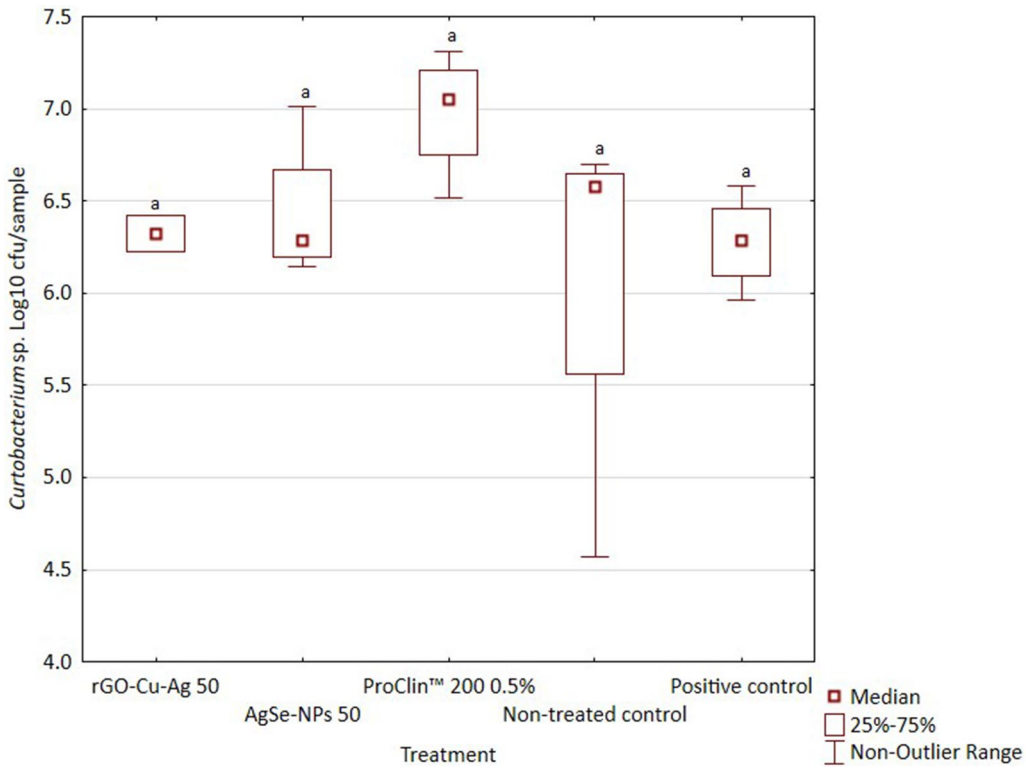

Fig. 4 Quantification of *Curtobacterium* sp. using qPCR in samples obtained from the surface of tissue culture medium treated with nanomaterials at a concentration of 1 × MBC (50 mg L^{-1} Ag). The same letters indicate no significant difference according to Tukey's test ($p < 0.05$)

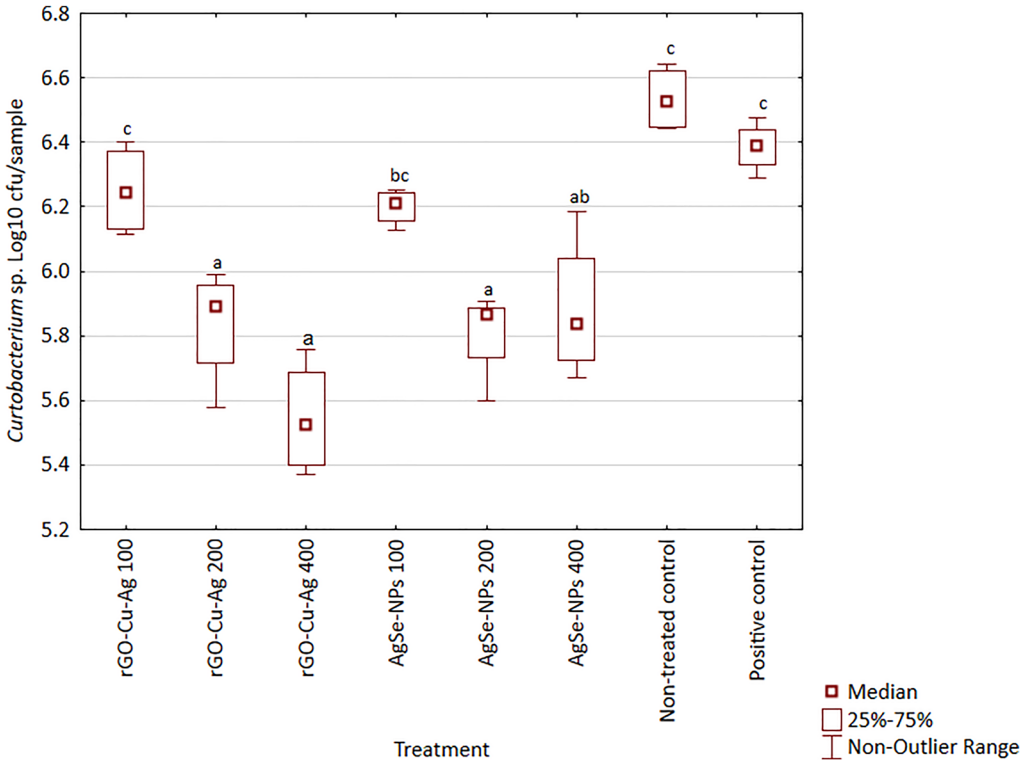

Fig. 5 Quantification of *Curtobacterium* sp. using qPCR in samples obtained from the surface of tissue culture medium treated with nanomaterials at concentrations of 2 ×–8 × MBC (100–400 mg L^{-1} Ag). The same letters indicate no significant difference according to Tukey's test ($p < 0.05$)

that of *Curtobacterium flaccumfaciens*; however, whole-genome sequencing confirmed that *Curtobacterium* sp. A7_M15 is not *Curtobacterium flaccumfaciens*. The phylogeny based on the 1190 bp part of 16S rDNA indicates the highest similarity of *Curtobacterium* sp. isolate A7_M15 to *Curtobacterium* sp. isolate BH-2-1-1 (Fig. 2). The biochemical characteristics of the *Curtobacterium sp.* A7_M15 isolate are listed in Additional file 2: Table S1.

Genomic information of *Curtobacterium* sp. A7_M15

The genome of *Curtobacterium* sp. A7_M15 reported here has been deposited in GenBank under Acc. No. JAUZED000000000 (BioProject No. PRJNA1000426). De novo assembly of *Curtobacterium* sp. A7_M15 resulted in a genome size of 3,833,925 bp, G+C content of 71.08%, and 231 contigs, with a scaffold length at which 50% of the total assembly length is covered (N50) value of 28,780.

Minimum bactericidal concentration of nanomaterials

The antibacterial activity of the tested nanomaterials against *Curtobacterium* sp. A7_M15 was evaluated, and minimum bactericidal concentrations (MBCs) were determined. The nanomaterials varied in effectivity, and the lowest MBC was observed for rGO-Cu-Ag (50.00 mg L^{-1} Ag and 32.50 mg L^{-1} Cu) and AgSe-NPs (50.00 mg L^{-1} Ag and 30.83 mg L^{-1} Se) (Fig. 3c). rGO-Cu had bactericidal activity at a concentration of 500 mg L^{-1}, and rGO-Zn was not effective even at a concentration of 1000 mg L^{-1} (Fig. 3a, b). Bacterial growth was present after treatment with AgNPs_1 and AgNPs_2 at a concentration of 50 mg L^{-1}, which was the highest achievable concentration in the case of these two nanoparticles (Fig. 3d).

Bacterial growth inhibition on tissue culture medium

The effectiveness of the tested nanomaterials in the inhibition of bacterial contamination on plant growth medium was evaluated based on the number of plaques present on the medium surface and is expressed as a percentage reduction in the number of plaques compared to the positive control (Table 2). Complete inhibition was observed for both nanomaterials at concentrations of 100, 200 and 400 mg L^{-1}. rGO-Cu-Ag at a concentration of 50 mg L^{-1} reduced bacterial contamination by 45% and AgSe-NPs at the same concentration by 30%. The use of ProClin 200™ at the recommended concentration of 0.5% (v/v) resulted in a 10% reduction in bacterial contamination. The treatment was considered effective when 100% bacterial growth inhibition was observed.

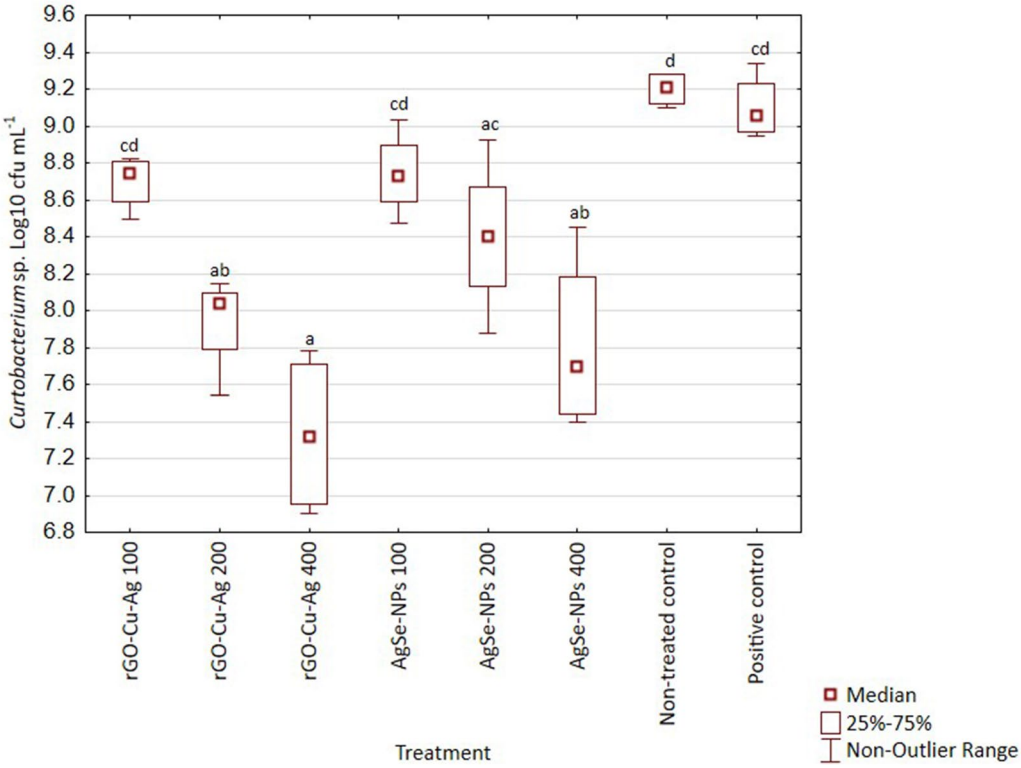

Fig. 6 Quantification of *Curtobacterium* sp. using the method of enumeration of living bacteria on medium in samples obtained from the surface of tissue culture medium treated with nanomaterials at concentrations of 2 ×–8 × MBC (100–400 mg L^{-1} Ag). The same letters indicate no significant difference according to Tukey's test ($p < 0.05$)

Bacterial growth was also observed on noninoculated variants, which is probably a consequence of naturally occurring internal contamination of tested plants.

Quantification of *Curtobacterium* sp. on plant tissue medium

The effectiveness of the tested nanomaterials in the reduction of *Curtobacterium* sp. quantity on the surface of plant tissue medium was evaluated using two approaches: qPCR absolute quantification and determination of living bacteria by cfu enumeration on culture medium. The results from qPCR show that none of the treatments with nanomaterials at 1 × MBC (50 mg L^{-1}) or 0.5% ProClin™ 200 was effective in reducing the *Curtobacterium* sp. cfu number in comparison to the positive control (Fig. 4). Subsequently, in the experiment, where higher concentrations of 2 ×–8 × MBC were used, qPCR absolute quantification confirmed that both nanomaterials at concentrations of 200 and 400 mg L^{-1} significantly limited the *Curtobacterium* sp. cfu number in comparison to the positive control (Fig. 5). The strongest decrease was observed after treatment with 400 mg L^{-1} of rGO-Cu-Ag, where the *Curtobacterium* sp. cfu number was by 85% lower than that in the positive control. A concentration of 200 mg L^{-1} of rGO-Cu-Ag and AgSe-NPs reduced the cfu quantity by 70% and 73%, respectively, in comparison to the positive control and was significantly more effective than 100 mg L^{-1}.

The results obtained by enumeration of living bacteria in samples corresponded to the results of qPCR quantification in the experiment where nanomaterial concentrations of 2 ×–8 × MBC were used. In the experiment with 1 × MBC, colonies grown on Petri dishes were too numerous and uncountable; therefore, quantification by this approach was not possible. For rGO-Cu-Ag 400 mg L^{-1}, similar results were obtained by enumeration of *Curtobacterium* sp. colonies as from qPCR quantification, where the cfu number was the lowest and reduced by 98% in comparison to the positive control (Fig. 6). Additionally, 200 mg L^{-1} of rGO-Cu-Ag significantly decreased living *Curtobacterium* sp. quantity in comparison to the positive control (93%). In the case of AgSe-NPs, the concentration of 400 mg L^{-1} was more efficient than 100 mg L^{-1}, reducing *Curtobacterium* sp. by 92% in comparison to the positive control. No statistically significant difference was observed between the tested nanomaterials at the same concentrations, regardless of the method used for *Curtobacterium* sp. cfu quantification. Both approaches showed

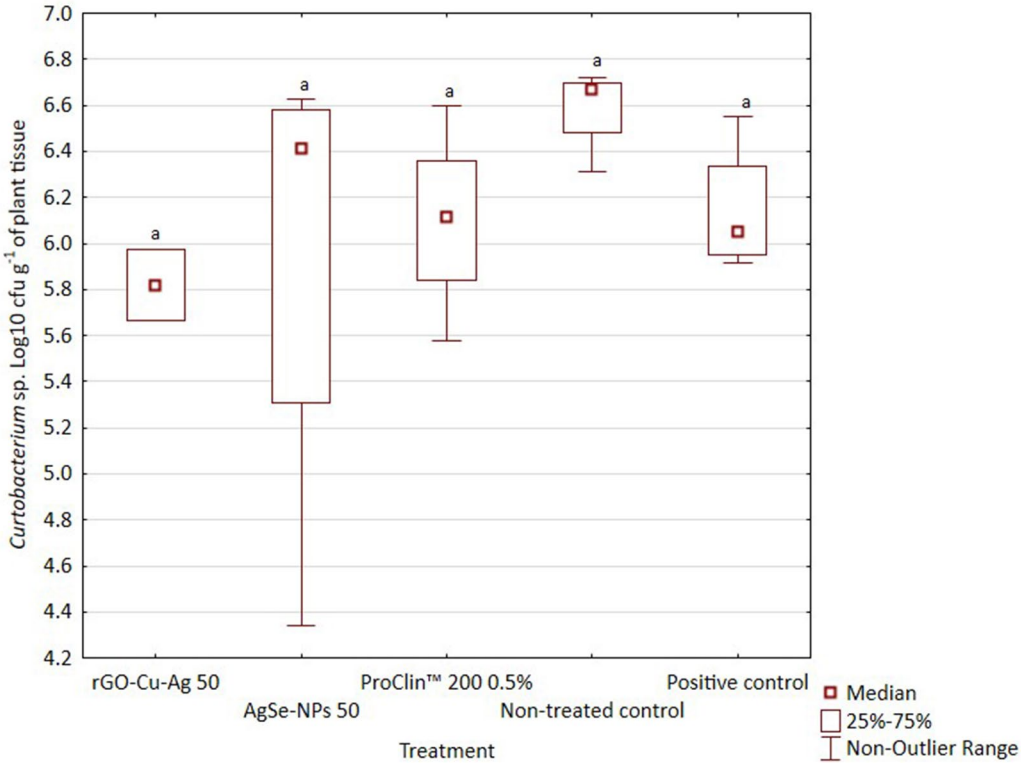

Fig. 7 Quantification of *Curtobacterium* sp. using qPCR in plants grown on medium treated with nanomaterials at a concentration of 1 × MBC (50 mg L^{-1} Ag). The same letters indicate no significant difference according to Tukey's test ($p < 0.05$)

that *Curtobacterium* sp. was present in non-treated control samples.

Quantification of Curtobacterium sp. in plants treated with nanomaterials

The effect of applied nanomaterials on the quantity of *Curtobacterium* sp. in explants was investigated and analyzed using qPCR. Donor plants were tested for the presence of *Curtobacterium* sp. in tissues, and in all samples, the bacterium was detected. Treatments with both nanomaterials at almost all concentrations and 0.5% ProClin™ 200 did not significantly affect *Curtobacterium* sp. quantity in the tested plants (Figs. 7 and 8), with the exception of 400 mg L^{-1} AgSe-NPs, where the number of bacteria was higher than that in all other variants.

Effect of nanomaterial treatments on in vitro plant mass

After a 3-week growth period, in vitro Gisela 5 rootstock plants were collected from the medium and weighed. In the experiment where a nanomaterial concentration of 1 × MBC was applied, nanomaterials and 0.5% ProClin™ 200 did not significantly affect plant mass in comparison to the non-treated control and positive control (Fig. 9). In the experiment where nanomaterial concentrations of 2 ×, 4 × and 8 × MBC were applied, plants from the positive control had the highest mass, but it was not significantly higher than that of non-treated control plants (7.77 *g* and 7.28 *g*, respectively) (Fig. 10). After treatments with both nanomaterials, a trend of decreasing plant mass corresponding to increasing concentration was observed; however, treatment with rGO-Cu-Ag at all tested concentrations, as well as AgSe-NPs at a concentration of 100 mg L^{-1}, did not significantly reduce plant mass in comparison to the positive control and non-treated control. A significant decrease in mass, in comparison to the non-treated control and positive control, was observed for plants treated with 200 and 400 mg L^{-1} AgSe-NPs (4.18 and 2.54 *g*, respectively). Plants treated with 400 mg L^{-1} AgSe-NPs also had significantly lower mass than plants treated with 100 mg L^{-1} AgSe-NPs (6.77 *g*).

Effect of nanomaterial treatments on the size of the surface covered by plants

The effect of the tested nanomaterials on in vitro plant development was evaluated by determining the surface covered by plants. In the experiment with nanomaterial treatment at a concentration of 1 × MBC, the positive control plants covered the largest surface area

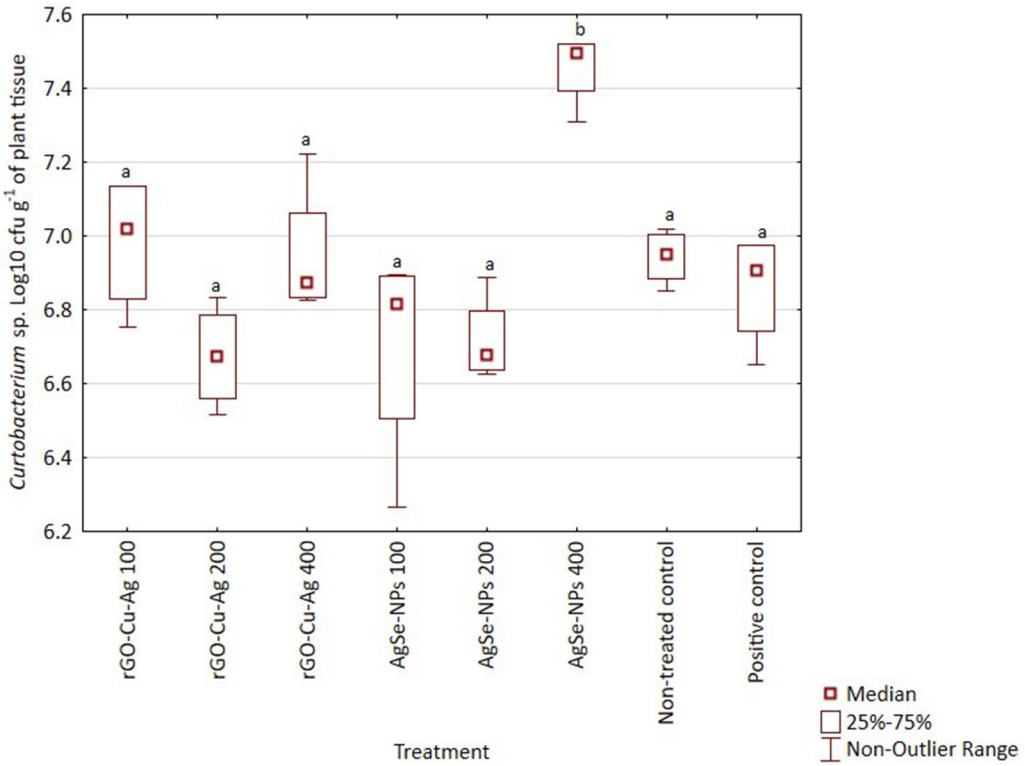

Fig. 8 Quantification of *Curtobacterium* sp. using qPCR in plants grown on medium treated with nanomaterials at concentrations of 2 ×–8 × MBC (100–400 mg L^{-1} Ag). The same letters indicate no significant difference according to Tukey's test ($p < 0.05$)

(41.21 cm^2) (Fig. 11). The surface covered by plants treated with 50 mg L^{-1} of rGO-Cu-Ag and AgSe-NPs, 0.5% ProClin™ 200, and non-treated plants was similar (30.11, 27.81, 32.06 and 32.88 cm^2, respectively), and it was significantly smaller than that of the positive control. In the second experiment, where concentrations of 2 ×–8 × MBC were used, a decrease in the surface covered by plants with increasing concentration was observed for both nanomaterials (Fig. 12); however, only plants treated with 400 mg L^{-1} of rGO-Cu-Ag and AgSe-NPs (31.89 and 29.87 cm^2) covered a significantly smaller surface than both the positive control and non-treated control (38.52 and 38.31 cm^2) (Fig. 13). AgSe-NPs at a concentration of 400 mg L^{-1} significantly reduced the surface covered by plants in comparison with 100 and 200 mg L^{-1}. Comparison between treatments with the same concentrations of two nanomaterials shows no significant difference between surfaces covered by plants.

Phytotoxicity of nanomaterials and effect on plant dry weight

The possible negative effect of the tested nanomaterials on plants developed in in vitro cultures was evaluated in comparison to non-treated control plants. No visible phytotoxic effect was observed on plants, regardless of the applied concentrations. Plants collected after the growth period were analyzed to determine the dry weight content. Nanomaterials at all tested concentrations did not affect the dry weight content of plants (Fig. 14).

Discussion

Micropropagation is one the most effective approaches for obtaining a large number of highly uniform plants in a short time. Microbial contamination poses a high risk during all stages of in vitro plant production. Even microorganisms that are nonpathogenic or even beneficial in vivo can have a critical impact on plant tissue cultures, and for successful maintenance of in vitro cultures, it is necessary to prevent contamination [49].

The spectrum of bacterial species contaminating plant in vitro cultures is very wide depending on different factors, such as plant species, culture medium and source of contamination [6, 32, 50]. In the present study, tissue cultures of six *Prunus* rootstock genotypes were screened for the presence of bacterial colonies, and six *Curtobacterium* sp. isolates were identified. This finding is consistent with our previous results obtained using High-Throughput Amplicon Sequencing, showing the presence of the genus *Curtobacterium* in contaminated *Prunus* rootstock tissue cultures [32]. *Curtobacterium*

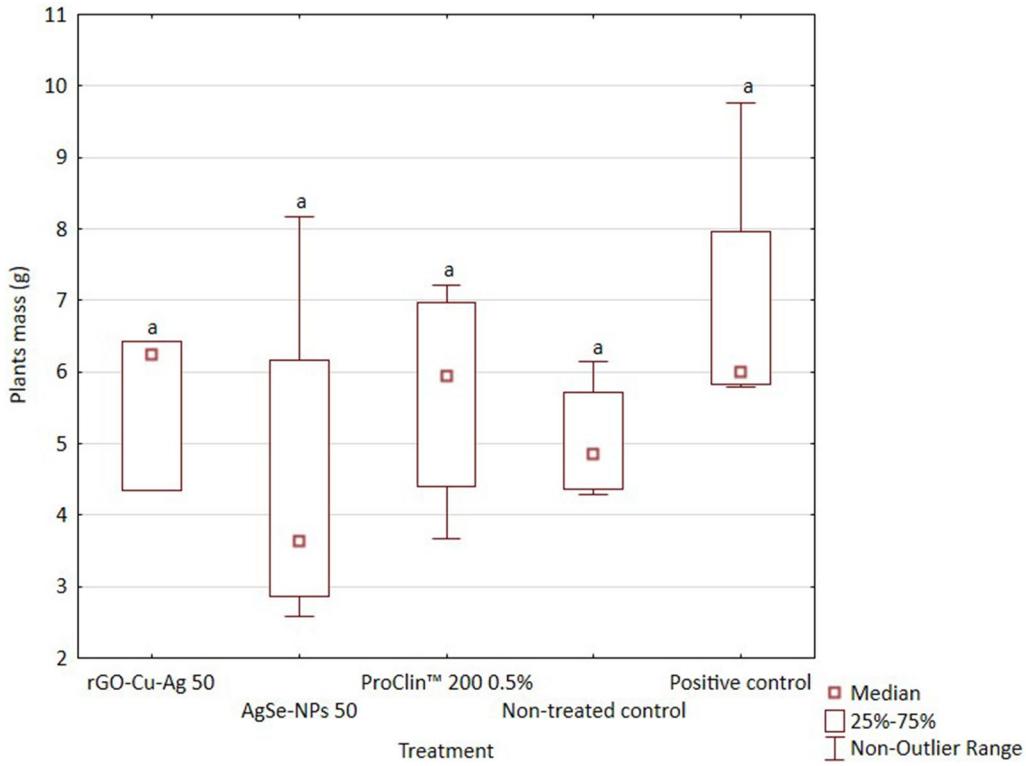

Fig. 9 Mass (g) of Gisela 5 rootstock in vitro plants treated with nanomaterials at a concentration of 1 × MBC (50 mg L^{-1} Ag). The same letters indicate no significant difference according to Tukey's test ($p < 0.05$)

spp. were also identified as contaminants of mint in vitro cultures [51], and bacterial colonies appearing on the medium surface of *Pancratium maritimum* L. explants were isolated and identified as *Curtobacterium flaccumfaciens* by Tumbarski, Georgiev [52]. The results obtained in this study therefore probably extend to in vitro cultures of other plant species besides *Prunus* sp. *Curtobacterium* spp. were also identified in the in vitro culture of *Prunus yedoensis*, where they initially acted as endophytic organisms but subsequently caused unwanted shoot tip necrosis after outgrowing the culture media [53]. The fact that overgrowth of endophytes in some tissue cultures may disrupt normal shoot tip growth and proliferation was also referred to by Cantabella, Teixidó [54], who recommend using endophyte-free cultures to achieve smooth plant micropropagation. According to Orlikowska, Nowak [2], bacterial plaques on media can change the medium composition as well as the composition of the atmosphere in the vessels, which may negatively influence plant culture growth. On the other hand, the promotion of plant development by endophytic bacteria in the case of their presence in in vitro cultures was also observed. Within the range of *Curtobacterium* spp., the positive effect of *Curtobacterium pusillum* presence in tissue cultures was reported by Zawadzka, Trzcinski [55], who observed stimulated axillary shoot formation in different plant species cultivated in vitro. Such observations suggest that the exact effect of *Curtobacterium* sp. on our donor Gisela 5 plants would require more focused characterization; however, the tendency of our particular isolate A7_M15 to form unwanted bacterial plaques on the media is obvious just from the beginning of our experiment.

The identification of occurring bacteria is an important part of the search for suitable measures and can help to select the appropriate antibacterial agent. Our six *Curtobacterium* sp. isolates were identified with high mutual similarity based on 16S rRNA sequencing. Regarding the phylogeny based on the 1190 bp part of 16S rDNA (Fig. 2), the *Curtobacterium* sp. isolate A7_M15 is the most similar to *Curtobacterium* sp. isolate BH-2-1-1, which is the biofilm-forming *Curtobacterium* sp. isolated from lettuce (*Lactuca sativa* L.) originating from a conventional field in Norway [56]. The genome of the Norwegian isolate is 3.8 Mb and contains 3 662 genes, 3 576 protein-coding sequences and 59 noncoding sequences. The Czech *Curtobacterium* sp. isolate A7_M15 is 3.8 Mb in size, with 3 725 genes, 3 626 protein-coding sequences and 56 noncoding sequences. Based on endophytic and

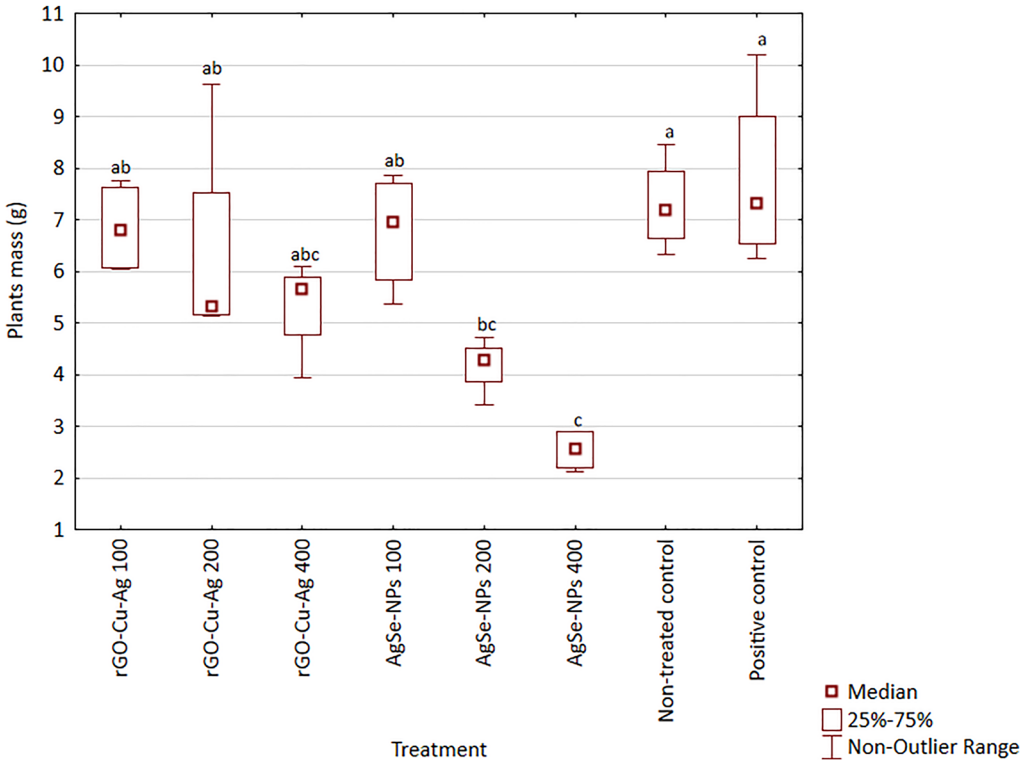

Fig. 10 Mass (g) of Gisela 5 rootstock in vitro plants treated with nanomaterials at concentrations of 2 ×–8 × MBC (100–400 mg L^{-1} Ag). The same letters indicate no significant difference according to Tukey's test ($p < 0.05$)

yellow-pigmented biofilm-forming features, these two bacterial strains are very similar to each other.

Crucial for limiting the losses caused by the presence of microorganisms in tissue cultures is the selection of disinfectants with high effectiveness but also without phytotoxic action on sensitive developing tissues. Disinfectants such as ethanol, sodium hypochlorite, mercury chloride or antibiotics are usually applied to plant material in in vitro cultures; however, they can have negative side effects [57–60], including the development of resistant strains of microbial contaminants in the case of antibiotic overuse [61, 62]. In the present study, we tested two nanocomposites as alternatives to eliminate bacterial growth on the surface of tissue culture medium, and we also analyzed their effect on explant development and in planta *Curtobacterium* sp. quantity. The antibacterial activity of nanomaterials could be explained by several mechanisms of their functionality that were currently reviewed by Xie, Gao [63]. The principal modes of action are based on the release of metal ions as well as the direct contact of nanoparticles with cell structures [64, 65]. Following the abovementioned properties, the antibacterial effect can be enhanced through the synergistic effect of composite nanomaterials [66]. Cruces, Arancibia-Miranda [67] published the effective antibacterial effect of Cu/Ag NPs against *Escherichia coli* and *Staphylococcus aureus.* Perdikaki, Galeou [68] demonstrated the bactericidal effect of a Ag/Cu bimetallic nanocomposite against *E. coli,* while Ag- and Cu-based monometallic NPs only reduced bacterial growth. Reduced graphene oxide (rGO) decorated by sulfur and selenium nanoparticles displayed inhibitory action against *S. aureus* and *Enterococcus faecalis* [27]. In a study by Mostafa, El-Sayyad [69], Ag-Se NPs showed antibacterial activity against various strains of pathogenic bacteria. Such a tendency was also confirmed by our results, when out of the six tested nanomaterials, the rGO-Cu-Ag and AgSe-NPs as bimetallic nanoparticles proved to be the most effective.

rGO-Cu-Ag and AgSe-NPs were selected as the most effective nanomaterials based on the MBC results. These nanocomposites have also been proven to have antimicrobial effects in other works [26, 44]. Nevertheless, the MBC (50 mg L^{-1}) determined by testing the nanocomposites against the pure culture of the *Curtobacterium* sp. isolate A7_M15 was not effective when used in the experiment with the plant tissue. In fact, despite the long-term exposure of the young plant material to the 1 × MBC nanomaterial concentration, bacterial cells were not eliminated, and their amount

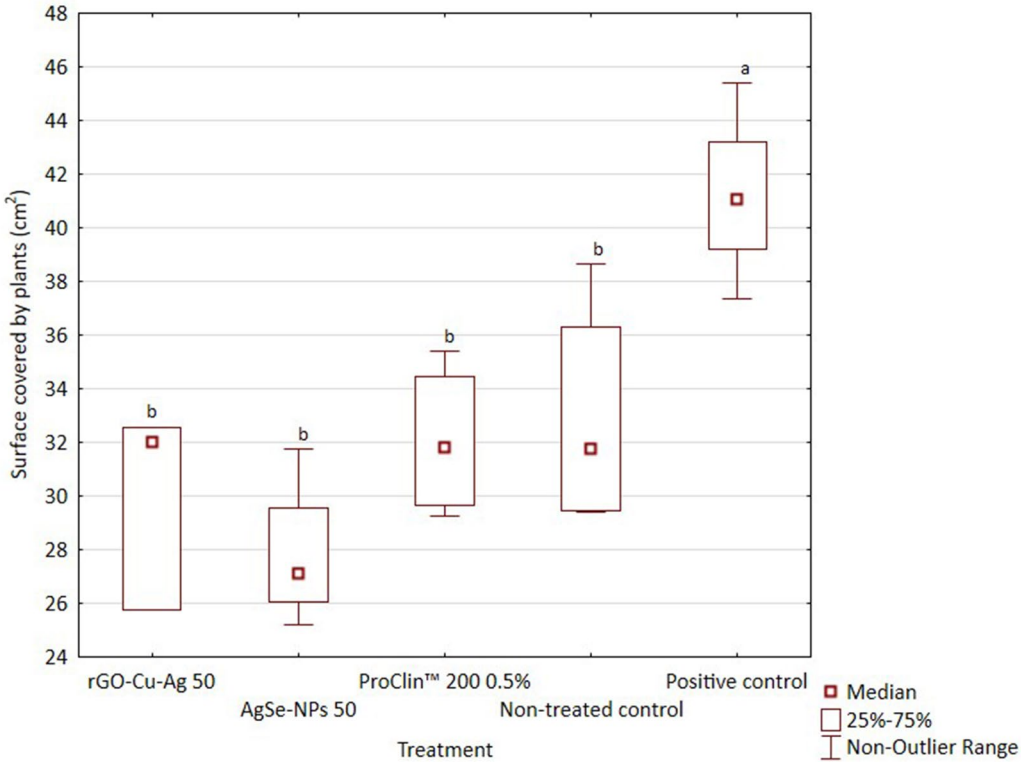

Fig. 11 Surface (cm^2) covered by Gisela 5 rootstock in vitro plants treated with nanomaterials at a concentration of 1 × MBC (50 mg L^{-1} Ag). The same letters indicate no significant difference according to Tukey's test ($p < 0.05$)

remained similar to that in the control. This could be explained by the fact that *Curtobacterium* was already detected in donor plant material, and thus, the natural presence of this bacterium within plant tissues could provide a source of inoculum that is difficult to disrupt or exhaust. This interpretation is further confirmed by the fact that *Curtobacterium* spp. is described as a relatively common part of the microbiome in stone fruits [70, 71] and that in *Prunus* spp. *Curtobacterium* spp. have even been described as not epiphytic but exclusively endophytic [72]. On the other hand, an increase in the concentration of nanocomposites induced a significant reduction in *Curtobacterium* sp. contamination. Both nanocomposites showed 100% inhibition of bacterial plaque formation on culture medium at concentrations of 100, 200 and 400 mg L^{-1} Ag (2 ×–8 × MBC). The treatments with 200 mg L^{-1} Ag resulted in a reduction in living *Curtobacterium* sp. quantity on culture medium by 92% in the case of rGO-Cu-Ag and a decrease in cfu number assessed using qPCR by 73% in the case of AgSe-NPs. This concentration simultaneously had no retardation effect on explants. Up to a 98% reduction in living bacteria was observed after treatment with nanocomposites at a concentration of 400 mg L^{-1}.

The ascertained antibacterial effect of the tested nanomaterials on *Curtobacterium* sp. was limited to the medium surface, and no significant decrease in the quantity of this bacterium was determined in explants. The reason is likely to be the disruption of one of the mechanisms involved in the process of nanoparticle distribution in the plant [73]. Nanomaterials are showing various bioavailability to plant systems what is modulated by different nanomaterials features related to their type, size, surface coating, borne energy, as well as their susceptibility to agglomeration and dissolution [74]. These chemical and physical properties influence processes as adsorption, internalization and intracellular fate, undergoing with correlation to environmental factors. Moreover, the genotype and anatomy of plant are other factors determining the ability and effectiveness of nanomaterials uptake [75]. These make every nanomaterials–plant interaction very complex and challenging for evaluation. The impact of nanomaterials on plants can be related either to their ability to release ions or being incorporated in plants tissues. After the uptake by plants, nanomaterials are submitted to plant-mediated transformation [76]. It may concern changes in their structure and chemistry [77], formation of complexes with other elements [78], size modification [76]. Except uptake, transport and

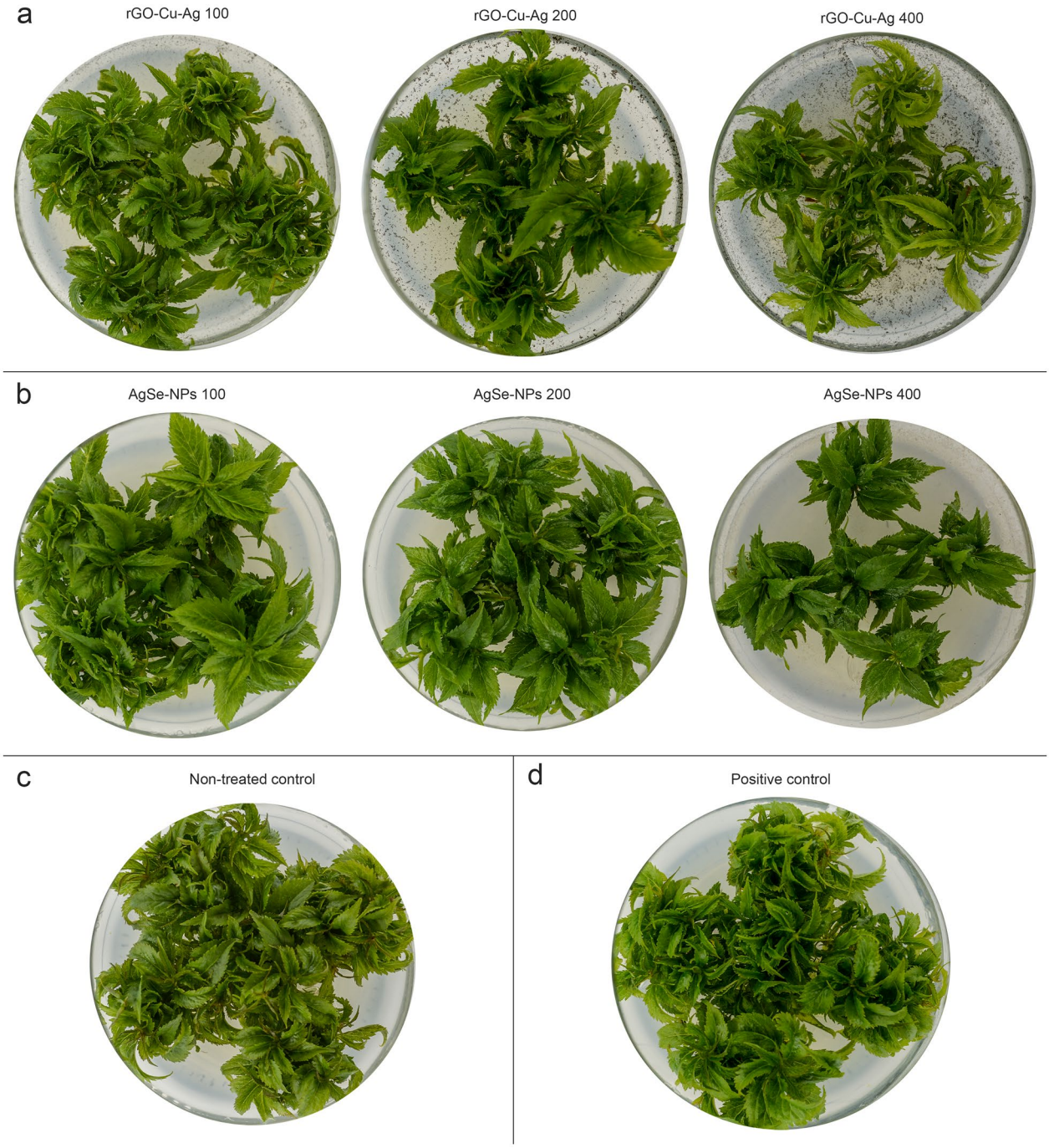

Fig. 12 Gisela 5 explants after 3 weeks of growth on medium treated with rGO-Cu-Ag (**a**) and AgSe-NPs (**b**) at concentrations of 2 ×–8 × MBC (100–400 mg L^{-1} Ag) compared with the non-treated control (**c**) and positive control (**d**)

accumulation by plants, other issues should be included in the risk assessment of nanomaterials when introducing them to plant production sector, as life cycle analysis, bio-distribution and access to the food chain [79].

Specifically, in the case of rGO-Cu-Ag, the inability to eliminate *Curtobacterium* sp. in planta could be explained by the fact that the Ag and Cu NPs are locally immobilized on the relatively large rGO sheets, which prevents the translocation of Cu and Ag ions into the

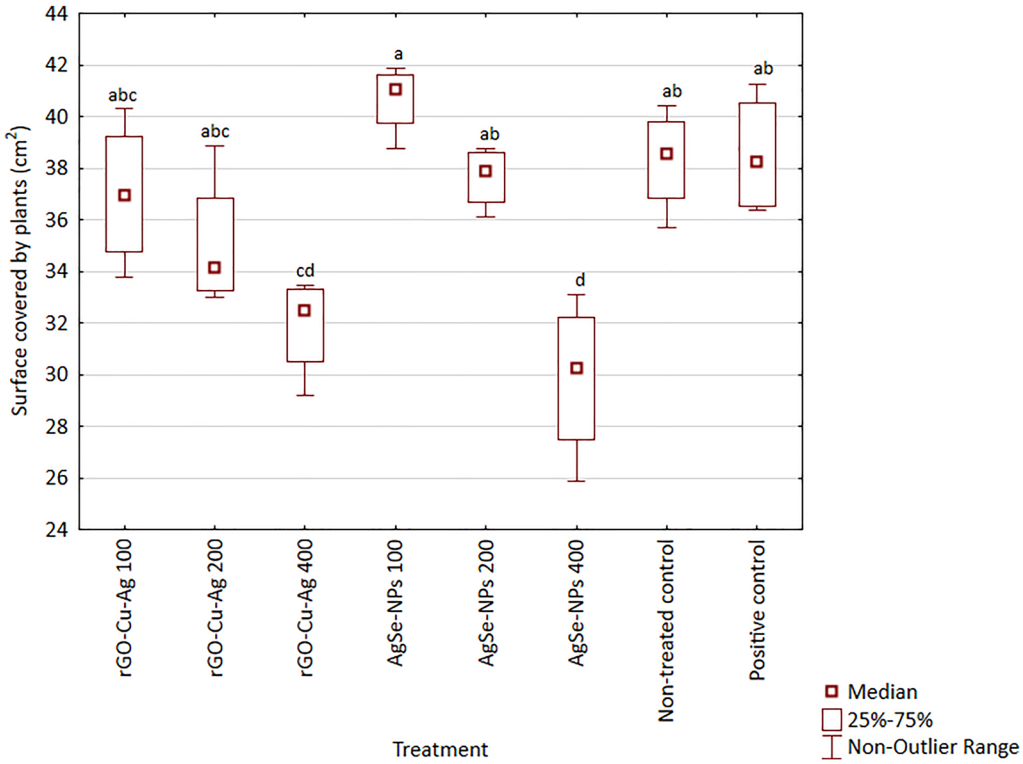

Fig. 13 Surface (cm^2) covered by Gisela 5 rootstock in vitro plants treated with nanomaterials at concentrations of 2 ×–8 × MBC (100–400 mg L^{-1} Ag. The same letters indicate no significant difference according to Tukey's test ($p < 0.05$)

plant tissues [80]. Moreover, the translocation ability of graphene-based nanomaterials can vary between different plant organs and species [80–82]. Some studies revealed that NPs can be trapped or aggregated on the surfaces or inside the plant tissues [83, 84], which could also reduce the efficiency of the used NPs in terms of eliminating internal *Curtobacterium* sp. occurrence in plants.

The applicability of nanomaterials for reducing bacterial contamination must also be assessed with respect to possible adverse effects on plants. Different effects of nanoparticles have been reported, i.e., from beneficial impacts on plant growth to retarded growth of treated plants [73]. In our experiment, rGO-Cu-Ag and AgSe-NPs were used for in vitro plant treatment, and the effect on explant growth through three parameters—plant mass, plant dry weight and surface of media covered by plants—was assessed. As reported, graphene-based nanomaterials can positively and negatively affect plant growth [85, 86]; however, no positive impact of the treatment was observed on any measured growth parameters in the present study. In their studies, Wang, Li [80], Arab, Yadollahi [87], Du, Zhang [88], Zhang, Gao [89] noted an undesirable effect of nanosilver on the viability of stone fruit rootstock buds at a concentration of 200 mg L^{-1} and increasing viability at a concentration of 100 mg L^{-1}. No negative effect of nanosilver at concentrations up to 100 mg L^{-1} was mentioned Abdi, Salehi [18], which is similar to our results. In the case of copper, Bao et al. [20] published the positive effect of CuNPs (100–300 mg L^{-1}) application on *Begonia x tuberhybrida* Voss in vitro cultures. In our treatments, the copper content ranged from 32.50 to 260 mg L^{-1} (1 ×–8 × MBC). Nanoselenium at doses up to 4 mg L^{-1} positively impacted biomass accumulation in the in vitro culture of bitter melon (*Momordica charantia* L.) seedlings; however, higher Se concentrations (10–50 mg L^{-1}) led to phytotoxic effects [90]. Analogous results were published by Sotoodehnia-Korani, Iranbakhsh [91] with in vitro cultures of *Capsicum annuum* L. According to our observations, the lowest Se concentration that had a negative impact on plants was 123.34 mg L^{-1} (200 mg L^{-1} Ag), which reduced explant mass but not dry weight or surface covered by plants. The only parameter that was not affected by the tested nanomaterials at any concentration was plant dry weight. For the explant mass, we observed a reduction only after treatment with AgSe-NPs at concentrations of 200 and 400 mg L^{-1}. Thus, unfortunately, we did not observe a synergistic effect when the reduction of bacterial

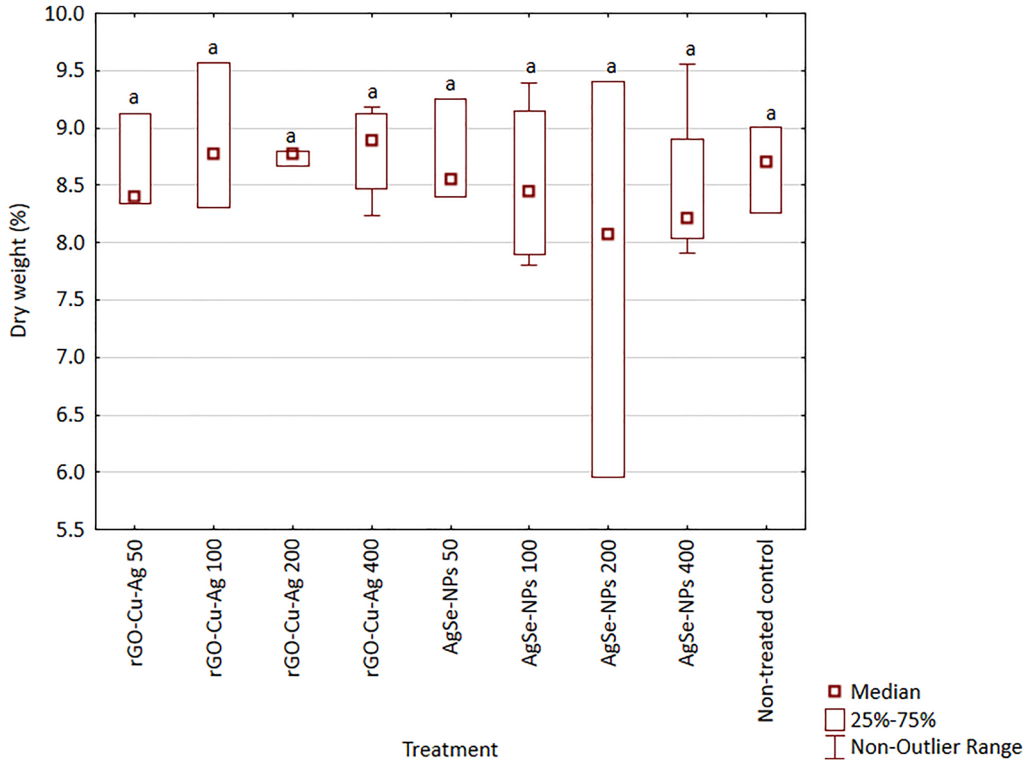

Fig. 14 Dry weight (%) of plants treated with 1 × MBC to 8 × MBC (50–400 mg L^{-1} Ag). The same letters indicate no significant difference according to Tukey's test ($p < 0.05$)

contamination would lead to a higher growth of plant tissues treated with nanomaterials.

Conclusions

Bacterial contaminants present on in vitro cultures of different *Prunus* rootstocks were isolated and identified as *Curtobacterium* sp. The genome of the *Curtobacterium* sp. A7_M15 isolate has been deposited in GenBank under Acc. No. JAUZED000000000 (BioProject Acc. No. PRJNA1000426). Two nanocomposites, rGO-Cu-Ag and AgSe-NPs, at concentrations of 100, 200 and 400 mg L^{-1} Ag effectively prevented visible bacterial growth on Gisela 5 rootstock in vitro cultures. A concentration of 200 mg L^{-1} of both nanocomposites significantly reduced *Curtobacterium* sp. quantity on the surface of plant tissue medium and did not reduce the surface covered by plants or plant dry weight. *Curtobacterium* sp. was detected in all donor plant materials, which suggests its endophytic character, and the quantity of this bacterium in plant tissues was not decreased even after treatment with the tested nanomaterials. To summarize, the results of this work indicate the potential use of rGO-Cu-Ag and AgSe-NPs at a concentration of 200 mg L^{-1} as preventive agents with strong activity against bacterial contamination occurring during in vitro plant production and without a negative impact on explant development. It is therefore possible to state nanocomposites as perspective for this application however, it is necessary to consider optimization of the cost of such a treatment in a large-scale use, taking as an aim to minimize the treatment cost below economical losses caused by microbial contaminations. Extension of effectivity evaluation to wider bacterial contaminants spectrum should be performed in the experiments following this study.

Abbreviations

rGO	Reduced graphene oxide
rGO-Zn	Reduced graphene oxide combined with zinc
rGO-Cu	Reduced graphene oxide combined with copper
rGO-Cu-Ag	Reduced graphene oxide combined with copper and silver
AgSe-NPs	Silver and selenium nanocomposite
AgNPs_1	Silver nanoparticles 1
AgNPs_2	Silver nanoparticles 2
cfu	Colony forming unit
MBC	Minimum bactericidal concentration
PBS	Phosphate-buffered saline
PCR	Polymerase chain reaction
LA	Luria agar
LB	Luria broth

Supplementary Information

The online version contains supplementary material available at https://doi.org/10.1186/s40538-024-00536-6.

Additional file 1. Figure S1 (Monitoring the stability of AgSe-NPs over approximately one year) and Figure S2 (Monitoring the stability of rGO-Cu-Ag over approximately one year).

Additional file 2. Table S1 (Biochemical characteristics of the Curtobacterium sp. A7_M15 isolate).

Acknowledgements
The authors would like to thank Břetislav Křižan (Vitrotree by Battistini) for providing the samples, Jana Moudrá (Mendel University in Brno, Czech Republic) for the laboratory support and Milan Špetík (Mendel University in Brno, Czech Republic) for processing the images.

Author contributions
DT: conceptualization, methodology, writing—original draft, investigation, formal analysis, data curation, visualization, JP: methodology, writing—original draft, investigation, formal analysis, visualization, EH: methodology, writing—review and editing, JC: methodology, investigation, ZB: resources, methodology, writing—review and editing, LR: supervision, resources, writing—review and editing, TK: formal analysis, data curation, AE: writing—original draft, formal analysis, data curation, MB: supervision, conceptualization, writing—review and editing. All authors have read and agreed to the published version of the manuscript.

Funding
This article was created based on support from the project IGA-ZF/2022-SI1-005 (funded by Mendel University in Brno) and the project QK22010031 "Use of innovative potential of nanotechnology to enhance the rentability of selected areas of agricultural production" (funded by The Ministry of Agriculture of the Czech Republic).

Availability of data and materials
The datasets used and analyzed during the current study are available from the corresponding author on reasonable request. Newly generated sequences were deposited in the NCBI GenBank database under the following accession numbers: OR474083, OR474084, OR474085, OR474086, OR474087, OR474088. The genome of *Curtobacterium* sp. A7_M15 was deposited in the NCBI GenBank under Acc. No. JAUZED000000000 (BioProject No. PRJNA1000426).

Declarations

Ethics approval and consent to participate
Not applicable.

Competing interests
The authors declare no competing interests.

Author details
[1]Mendeleum—Institute of Genetics, Faculty of Horticulture, Mendel University in Brno, Valtická 334, 69144 Lednice, Czech Republic. [2]Department of Chemistry and Biochemistry, Faculty of AgriSciences, Mendel University in Brno, Zemědělská 1, 613 00 Brno, Czech Republic. [3]Department of Fruit Growing, Faculty of Horticulture, Mendel University in Brno, Valtická 337, 69144 Lednice, Czech Republic.

Received: 4 October 2023 Accepted: 9 January 2024
Published online: 25 January 2024

References

1. Leifert C, Woodward S. Laboratory contamination management: the requirement for microbiological quality assurance. Plant Cell Tiss Org. 1998;52(1–2):83–8.
2. Orlikowska T, Nowak K, Reed B. Bacteria in the plant tissue culture environment. Plant Cell Tiss Org. 2017;128(3):487–508.
3. Parzymies M, Pudelska K, Poniewozik M. The use of nano-silver for disinfection of Pennisetum alopecuroides plant material for tissue culture. Acta Sci Pol-Hortoru. 2019;18(3):127–35.
4. Carey SB, Payton AC, McDaniel SF. A method for eliminating bacterial contamination from in vitro moss cultures. Appl Plant Sci. 2015;3(1):1400086.
5. Cheong EJ, Na M, Jeong U. The effect of endophytic bacteria on in vitro shoot growth of Prunus yedoensis and its identification and elimination. In Vitro Cell Dev-Pl. 2020;56(2):200–6.
6. Moreno-Vazquez S, Larranaga N, Uberhuaga EC, Braga EJB, Perez-Ruiz C. Bacterial contamination of in vitro plant cultures: confounding effects on somaclonal variation and detection of contamination in plant tissues. Plant Cell Tiss Org. 2014;119(3):533–41.
7. Mbah EI, Wakil SM. Elimination of Bacteria from in Vitro Yam tissue cultures using antibiotics. J Plant Pathol. 2012;94(1):53–8.
8. Bhau BS, Wakhlu AK. Effect of some antibiotics on the in vitro morphogenetic response from callus cultures of Coryphantha elephantidens. Biol Plantarum. 2001;44(1):19–24.
9. Sandoval-Motta S, Aldana M. Adaptive resistance to antibiotics in bacteria: a systems biology perspective. Wiley Interdiscip Rev Syst Biol Med. 2016;8(3):253–67.
10. Hajipour MJ, Fromm KM, Ashkarran AA, de Jimenez Aberasturi D, de Larramendi IR, Rojo T, et al. Antibacterial properties of nanoparticles. Trends Biotechnol. 2012;30(10):499–511.
11. Spinoso-Castillo JL, Chavez-Santoscoy RA, Bogdanchikova N, Pérez-Sato JA, Morales-Ramos V, Bello-Bello JJ. Antimicrobial and hormetic effects of silver nanoparticles on in vitro regeneration of vanilla (Vanilla planifolia Jacks. ex Andrews) using a temporary immersion system. Plant Cell Tiss Organ Cult. 2017;129(2):195–207.
12. Wu Q, Huang KL, Sun HH, Ren HQ, Zhang XX, Ye L. Comparison of the impacts of zinc ions and zinc nanoparticles on nitrifying microbial community. J Hazard Mater. 2018;343:166–75.
13. Hamad A, Khashan KS, Hadi A. Silver nanoparticles and silver ions as potential antibacterial agents. J Inorg Organomet P. 2020;30(12):4811–28.
14. Baker C, Pradhan A, Pakstis L, Pochan DJ, Shah SI. Synthesis and antibacterial properties of silver nanoparticles. J Nanosci Nanotechno. 2005;5(2):244–9.
15. Bruna T, Maldonado-Bravo F, Jara P, Caro N. Silver nanoparticles and their antibacterial applications. Int J Mol Sci. 2021;22(13):7202.
16. Yimeng S, Huilun X, Ziming L, Kejun L, Chaima M, Xiangyu Z, et al. Copper-based nanoparticles as antibacterial agents. Eur J Inorg Chem. 2022. https://doi.org/10.1002/ejic.202200614.
17. Jin T, Sun D, Su JY, Zhang H, Sue HJ. Antimicrobial efficacy of zinc oxide quantum dots against listeria monocytogenes, salmonella enteritidis, and *Escherichia coli* O157:H7. J Food Sci. 2009;74(1):M46–52.
18. Abdi G, Salehi H, Khosh-Khui M. Nano silver: a novel nanomaterial for removal of bacterial contaminants in valerian (Valeriana officinalis L.) tissue culture. Acta Physiol Plant. 2008;30(5):709–14.
19. Parzymies M. Nano-silver particles reduce contaminations in tissue culture but decrease regeneration rate and slows down growth and development of aldrovanda vesiculosa explants. Appl Sci-Basel. 2021;11(8):3653.
20. Bao HG, Tung HT, Van HT, Bien L, Khai HD, Mai NTN, et al. Copper nanoparticles enhanced surface disinfection, induction and maturation of somatic embryos in tuberous begonias (Begonia x tuberhybrida Voss) cultured in vitro. Plant Cell Tiss Org. 2022;151(2):385–99.
21. Barjola A, Tormo-Mas MA, Sahuquillo O, Bernabe-Quispe P, Perez JM, Gimenez E. Enhanced antibacterial activity through silver nanoparticles deposited onto carboxylated graphene oxide surface. Nanomater-Basel. 2022;12(12):1949.
22. Liu SB, Zeng TH, Hofmann M, Burcombe E, Wei J, Jiang RR, et al. Antibacterial activity of graphite, graphite oxide, graphene oxide, and reduced graphene oxide: membrane and oxidative stress. ACS Nano. 2011;5(9):6971–80.
23. Alayande AB, Obaid M, Kim IS. Antimicrobial mechanism of reduced graphene oxide-copper oxide (rGO-CuO) nanocomposite films: the case of Pseudomonas aeruginosa PAO1. Mat Sci Eng C-Mater. 2020;109:110596.
24. Tu YS, Lv M, Xiu P, Huynh T, Zhang M, Castelli M, et al. Destructive extraction of phospholipids from *Escherichia coli* membranes by graphene nanosheets. Nat Nanotechnol. 2013;8(8):594–601.
25. Hui LW, Piao JG, Auletta J, Hu K, Zhu YW, Meyer T, et al. Availability of the basal planes of graphene oxide determines whether it is antibacterial. Acs Appl Mater Inter. 2014;6(15):13183–90.

26. Bytešníková Z, Pečenka J, Tekielska D, Kiss T, Švec P, Ridošková A, et al. Reduced graphene oxide-based nanometal-composite containing copper and silver nanoparticles protect tomato and pepper against Xanthomonas euvesicatoria infection. Chem Biol Technol Ag. 2022;9(1):84.
27. Niranjan R, Zafar S, Lochab B, Priyadarshini R. Synthesis and Characterization of sulfur and sulfur-selenium nanoparticles loaded on reduced graphene oxide and their antibacterial activity against gram-positive pathogens. Nanomater-Basel. 2022;12(2):191.
28. Romadanova NV, Tolegen AB, Kushnarenko SV, Zholdybayeva EV, Bettoni JC. Effect of plant preservative mixture (TM) on endophytic bacteria eradication from in vitro-grown apple shoots. Plants-Basel. 2022;11(19):2624.
29. Nadha HK, Salwan R, Kasana RC, Anand M, Sood A. Identification and elimination of bacterial contamination during in vitro propagation of Guadua angustifolia Kunth. Pharmacogn Mag. 2012;8(30):93–7.
30. Cassells AC. Pathogen and biological contamination management in plant tissue culture: phytopathogens, vitro pathogens, and vitro pests. Methods Mol Biol. 2012;877:57–80.
31. Fang JY, Hsu YR. Molecular identification and antibiotic control of endophytic bacterial contaminants from micropropagated Aglaonema cultures. Plant Cell Tiss Org. 2012;110(1):53–62.
32. Tekielska D, Peňázová E, Kovács T, Křižan B, Čechová J, Eichmeier A. Bacterial contamination of plant in vitro cultures in commercial production detected by high-throughput amplicon sequencing. Acta Univ Agric Silvic Mendelianae Brun. 2019;67(4):1005–14.
33. Evtushenko LI, Takeuchi M. The family Microbacteriaceae. In: Dworkin M, Falkow S, Rosenberg E, Schleifer K-H, Stackebrandt E, editors. The Prokaryotes: Archaea Bacteria: Firmicutes, Actinomycetes, vol. 3. New York: Springer, New York; 2006. p. 1020–98.
34. Osdaghi E, Young AJ, Harveson RM. Bacterial wilt of dry beans caused by Curtobacterium flaccumfaciens pv. flaccumfaciens: a new threat from an old enemy. Mol Plant Pathol. 2020;21(5):605–21.
35. Chase AB, Arevalo P, Polz MF, Berlemont R, Martiny JBH. Evidence for ecological flexibility in the cosmopolitan genus Curtobacterium. Front Microbiol. 2016;7:1874.
36. Klindworth A, Pruesse E, Schweer T, Peplies J, Quast C, Horn M, et al. Evaluation of general 16S ribosomal RNA gene PCR primers for classical and next-generation sequencing-based diversity studies. Nucleic Acids Res. 2013;41(1):e1.
37. Bankevich A, Nurk S, Antipov D, Gurevich AA, Dvorkin M, Kulikov AS, et al. SPAdes: a new genome assembly algorithm and its applications to single-cell sequencing. J Comput Biol. 2012;19(5):455–77.
38. Keller O, Kollmar M, Stanke M, Waack S. A novel hybrid gene prediction method employing protein multiple sequence alignments. Bioinformatics. 2011;27(6):757–63.
39. Li R, Li Y, Kristiansen K, Wang J. SOAP: short oligonucleotide alignment program. Bioinformatics. 2008;24(5):713–4.
40. Li R, Zhu H, Ruan J, Qian W, Fang X, Shi Z, et al. De novo assembly of human genomes with massively parallel short read sequencing. Genome Res. 2010;20(2):265–72.
41. Simpson JT, Wong K, Jackman SD, Schein JE, Jones SJ, Birol I. ABySS: a parallel assembler for short read sequence data. Genome Res. 2009;19(6):1117–23.
42. Lin SH, Liao YC. CISA: contig integrator for sequence assembly of bacterial genomes. PLoS ONE. 2013;8(3):e60843.
43. Đurović A, Stojanović Z, Bytešníková Z, Kravić S, Švec P, Přibyl J, et al. Reduced graphene oxide/ZnO nanocomposite modified electrode for the detection of tetracycline. J Mater Sci. 2022;57(9):5533–51.
44. Štůsková K, Pečenka J, Tekielska DA, Špetík M, Bytešníková Z, Švec P, et al. The in vitro effects of selected substances and nanomaterials against Diaporthe eres, Diplodia seriata and Eutypa lata. Ann Appl Biol. 2023;182(2):226–37.
45. Pečenka J, Bytešníková Z, Kiss T, Peňázová E, Baránek M, Eichmeier A, et al. Silver nanoparticles eliminate Xanthomonas campestris pv campestris in cabbage seeds more efficiently than hot water treatment. Mater Today Commun. 2021;27:102284.
46. Evseev P, Lukianova A, Tarakanov R, Tokmakova A, Shneider M, Ignatov A, et al. Curtobacterium spp. and Curtobacterium flaccumfaciens: phylogeny, Genomics-Based Taxonomy, pathogenicity, and diagnostics. Curr Issues Mol Biol. 2022;44(2):889–927.
47. Tamura K, Nei M. Estimation of the number of nucleotide substitutions in the control region of mitochondrial-DNA in humans and chimpanzees. Mol Biol Evol. 1993;10(3):512–26.
48. Kumar S, Stecher G, Li M, Knyaz C, Tamura K. MEGA X: molecular evolutionary genetics analysis across computing platforms. Mol Biol Evol. 2018;35(6):1547–9.
49. Klayraung S, Niamsup P, Poonnoy P, Topoonyanont N, editors. Diversity and control of bacterial contamination of plants propagated in temporary immersion bioreactor system. In: VI International Symposium on Production and Establishment of Micropropagated Plants 1155. 2015.
50. Fang J-Y, Hsu Y-R. Molecular identification and antibiotic control of endophytic bacterial contaminants from micropropagated Aglaonema cultures. Plant Cell Tiss Organ Cult (PCTOC). 2012;110(1):53–62.
51. Buckley PM, DeWilde TN, Reed BM. Characterization and identification of bacteria isolated from micropropagated mint plants. In Vitro Cell Dev Biol—Plant. 1995;31(1):58–64.
52. Tumbarski Y, Georgiev V, Nikolova R, Pavlov A. Isolation, identification and antibiotic susceptibility of Curtobacterium flaccumfaciens strain PM_YT from sea daffodil (Pancratium maritimum L.) shoot cultures. J Microbiol Biotechnol Food Sci. 2018;7(6):623.
53. Cheong EJ, Na M, Jeong U. The effect of endophytic bacteria on in vitro shoot growth of Prunus yedoensis and its identification and elimination. In Vitro Cell Dev Biol—Plant. 2020;56(2):200–6.
54. Cantabella D, Teixidó N, Solsona C, Casanovas M, Torres R, Dolcet-Sanjuan R. Acidification of the culture medium as a strategy to control endophytic contaminations in Prunus spp. rootstocks cultured in GreenTray TIS bioreactor. Sci Horticult. 2021;290:110521.
55. Zawadzka M, Trzcinski P, Nowak K, Orlikowska T. The impact of three bacteria isolated from contaminated plantcultures on in vitro multiplication and rooting of microshoots of four ornamental plants. J Horticult Res.2013;21(2):41–51.
56. Dees MW, Brurberg MB, Lysøe E. Complete genome sequence of the biofilm-forming Curtobacterium sp. strain BH-2–1–1, isolated from lettuce (Lactuca sativa) originating from a conventional field in Norway. Genom Data. 2016;10:135–6.
57. Cornu D, Michel MF. Bacteria contaminants in shoot cultures of Prunus avium L. Choice and phytotoxicity of antibiotics. Leuven: International Society for Horticultural Science (ISHS); 1987.
58. Leifert C, Camotta H, Waites W. Effect of combinations of antibiotics on micropropagated Clematis, Delphinium, Hosta, Iris and Photinia. Plant Cell, Tissue Organ Cult. 1992;29:153–60.
59. Dodds JH, Roberts LW. some inhibitory effects of gentamicin on plant tissue cultures. In Vitro. 1981;17(6):467–70.
60. da Silva Mendes AF, Cidade LC, de Oliveira MLP, Otoni WC, Soares-Filho WDS, Costa MGC. Evaluation of novel beta-lactam antibiotics in comparison to cefotaxime on plant regeneration of *Citrus sinensis* L. Osb. Plant Cell, Tissu Organ Cult (PCTOC). 2009;97(3):331–6.
61. Barbosa TM, Levy SB. The impact of antibiotic use on resistance development and persistence. Drug Resist Updates. 2000;3(5):303–11.
62. Levy SB. The challenge of antibiotic resistance. Sci Am. 1998;278(3):46–53.
63. Xie M, Gao M, Yun Y, Malmsten M, Rotello VM, Zboril R, et al. Antibacterial nanomaterials: mechanisms, impacts on antimicrobial resistance and design principles. Angew Chem Int Ed. 2023;62(17):e202217345.
64. Nisar P, Ali N, Rahman L, Ali M, Shinwari ZK. Antimicrobial activities of biologically synthesized metal nanoparticles: an insight into the mechanism of action. J Biol Inorg Chem. 2019;24(7):929–41.
65. Bondarenko O, Ivask A, Käkinen A, Kurvet I, Kahru A. Particle-cell contact enhances antibacterial activity of silver nanoparticles. PLoS ONE. 2013;8(5):e64060.
66. Prasad K, Lekshmi GS, Ostrikov K, Lussini V, Blinco J, Mohandas M, et al. Synergic bactericidal effects of reduced graphene oxide and silver nanoparticles against Gram-positive and Gram-negative bacteria. Sci Rep. 2017;7(1):1591.
67. Cruces E, Arancibia-Miranda N, Manquián-Cerda K, Perreault F, Bolan N, Azócar MI, et al. Copper/Silver bimetallic nanoparticles supported on Aluminosilicate Geomaterials as antibacterial agents. ACS Appl Nano Mater. 2022;5(1):1472–83.
68. Perdikaki A, Galeou A, Pilatos G, Karatasios I, Kanellopoulos NK, Prombona A, et al. Ag and Cu monometallic and Ag/Cu bimetallic

nanoparticle-graphene composites with enhanced antibacterial performance. Acs Appl Mater Inter. 2016;8(41):27498–510.
69. Mostafa HY, El-Sayyad GS, Nada HG, Ellethy RA, Zaki EG. Promising antimicrobial and antibiofilm activities of Orobanche aegyptiaca extract-mediated bimetallic silver-selenium nanoparticles synthesis: Effect of UV-exposure, bacterial membrane leakage reaction mechanism, and kinetic study. Arch Biochem Biophys. 2023;736:109539.
70. Janisiewicz WJ, Buyer JS. Culturable bacterial microflora associated with nectarine fruit and their potential for control of brown rot. Can J Microbiol. 2010;56(6):480–6.
71. Janisiewicz WJ, Jurick WM, Vico I, Peter KA, Buyer JS. Culturable bacteria from plum fruit surfaces and their potential for controlling brown rot after harvest. Postharvest Biol Technol. 2013;76:145–51.
72. Vasebi Y, Khakvar R, Vinatzer BA. Characterization of culturable epiphytic and endophytic bacteria of Prunus spp. and their potential for plant growth promotion and antagonistic activity against bacterial canker disease. J Plant Pathol. 2023. https://doi.org/10.1007/s42161-023-01342-z.
73. Wohlmuth J, Tekielska D, Čechová J, Baránek M. Interaction of the nanoparticles and plants in selective growth stages-usual effects and resulting impact on usage perspectives. Plants. 2022;11(18):2405.
74. von Moos N, Bowen P, Slaveykova VI. Bioavailability of inorganic nanoparticles to planktonic bacteria and aquatic microalgae in freshwater. Environ Sci-Nano. 2014;1(3):214–32.
75. Rastogi A, Zivcak M, Sytar O, Kalaji HM, He XL, Mbarki S, et al. Impact of metal and metal oxide nanoparticles on plant: a critical review. Front Chem. 2017;5:78.
76. Ahmed B, Rizvi A, Ali K, Lee J, Zaidi A, Khan MS, et al. Nanoparticles in the soil-plant system: a review. Environ Chem Lett. 2021;19(2):1545–609.
77. Zhang P, Ma YH, Zhang ZY, He X, Zhang J, Guo Z, et al. Biotransformation of ceria nanoparticles in cucumber plants. ACS Nano. 2012;6(11):9943–50.
78. Dimkpa CO, Latta DE, McLean JE, Britt DW, Boyanov MI, Anderson AJ. Fate of CuO and ZnO Nano- and Microparticles in the plant environment. Environ Sci Technol. 2013;47(9):4734–42.
79. Karimi M, Sadeghi R, Kokini J. Human exposure to nanoparticles through trophic transfer and the biosafety concerns that nanoparticle-contaminated foods pose to consumers. Trends Food Sci Tech. 2018;75:129–45.
80. Wang QH, Li C, Wang Y, Que X. Phytotoxicity of graphene family nanomaterials and its mechanisms: a review. Front Chem. 2019;7:292.
81. Chen J, Yang L, Li S, Ding W. Various physiological response to graphene oxide and amine-functionalized graphene oxide in wheat (Triticum aestivum). Molecules. 2018;23(5):1104.
82. Zhao S, Wang Q, Zhao Y, Rui Q, Wang D. Toxicity and translocation of graphene oxide in Arabidopsis thaliana. Environ Toxicol Pharmacol. 2015;39(1):145–56.
83. Tryfon P, Kamou NN, Mourdikoudis S, Karamanoli K, Menkissoglu-Spiroudi U, Dendrinou-Samara C. CuZn and ZnO Nanoflowers as nano-fungicides against Botrytis cinerea and Sclerotinia sclerotiorum: Phytoprotection, translocation, and Impact after foliar application. Materials. 2021;14(24):7600.
84. Lv J, Christie P, Zhang S. Uptake, translocation, and transformation of metal-based nanoparticles in plants: recent advances and methodological challenges. Environ Sci Nano. 2019;6(1):41–59.
85. Xie L-L, Chen F, Zou X-L, Shen S-S, Wang X-G, Yao G-X, et al. Graphene oxide and ABA cotreatment regulates root growth of *Brassica napus* L. by regulating IAA/ABA. J Plant Physiol. 2019;240:153007.
86. Guo X, Zhao J, Wang R, Zhang H, Xing B, Naeem M, et al. Effects of graphene oxide on tomato growth in different stages. Plant Physiol Biochem. 2021;162:447–55.
87. Arab MM, Yadollahi A, Hosseini-Mazinani M, Bagheri S. Effects of antimicrobial activity of silver nanoparticles on in vitro establishment of G×N15 (hybrid of almond×peach) rootstock. J Genet Eng Biotechnol. 2014;12(2):103–10.
88. Du S, Zhang P, Zhang R, Lu Q, Liu L, Bao X, et al. Reduced graphene oxide induces cytotoxicity and inhibits photosynthetic performance of the green alga Scenedesmus obliquus. Chemosphere. 2016;164:499–507.
89. Zhang M, Gao B, Chen J, Li Y. Effects of graphene on seed germination and seedling growth. J Nanopart Res. 2015;17(2):78.
90. Rajaee Behbahani S, Iranbakhsh A, Ebadi M, Majd A, Ardebili ZO. Red elemental selenium nanoparticles mediated substantial variations in growth, tissue differentiation, metabolism, gene transcription, epigenetic cytosine DNA methylation, and callogenesis in bittermelon (Momordica charantia); an in vitro experiment. PLoS ONE. 2020;15(7):e0235556.
91. Sotoodehnia-Korani S, Iranbakhsh A, Ebadi M, Majd A, Oraghi AZ. Selenium nanoparticles induced variations in growth, morphology, anatomy, biochemistry, gene expression, and epigenetic DNA methylation in Capsicum annuum; an in vitro study. Environ Pollut. 2020;265:114727.

Publisher's Note